Diversification of Transcriptional Regulation Determines Subfunctionalization of Paralogous Branched Chain Aminotransferases in the Yeast *Saccharomyces cerevisiae*

James González,* Geovani López,† Stefany Argueta,* Ximena Escalera-Fanjul,* Mohammed el Hafidi,‡ Carlos Campero-Basaldua,* Joseph Strauss,§ Lina Riego-Ruiz, and Alicia González*,1**

*Departamento de Bioquímica y Biología Estructural, Instituto de Fisiología Celular, and †Subdivisión de Medicina Familiar, División de Estudios de Posgrado, Facultad de Medicina, Universidad Nacional Autónoma de México, 04510 Ciudad de México, México, ‡Departamento de Biomedicina Cardiovascular, Instituto Nacional de Cardiología Ignacio Chávez, 14080 Ciudad de Méixco, México, §Fungal Genetics and Genomics Unit, Department of Applied Genetics and Cell Biology, University of Natural Resources and Life Sciences (BOKU), 1190 Tulln, Austria, and **División de Biología Molecular, Instituto Potosino de Investigación Científica y Tecnológica, 78216 San Luis Potosí, México

ORCID IDs: 0000-0002-7329-4025 (J.G.); 0000-0002-1276-5719 (A.G.)

ABSTRACT *Saccharomyces cerevisiae* harbors *BAT1* and *BAT2* paralogous genes that encode branched chain aminotransferases and have opposed expression profiles and physiological roles . Accordingly, in primary nitrogen sources such as glutamine, *BAT1* expression is induced, supporting Bat1-dependent valine–isoleucine–leucine (VIL) biosynthesis, while *BAT2* expression is repressed. Conversely, in the presence of VIL as the sole nitrogen source, *BAT1* expression is hindered while that of *BAT2* is activated, resulting in Bat2-dependent VIL catabolism. The presented results confirm that *BAT1* expression is determined by transcriptional activation through the action of the Leu3–α-isopropylmalate (α-IPM) active isoform, and uncovers the existence of a novel α-IPM biosynthetic pathway operating in a *put3*Δ mutant grown on VIL, through Bat2-Leu2-Leu1 consecutive action. The classic α-IPM biosynthetic route operates in glutamine through the action of the leucine-sensitive α-IPM synthases. The presented results also show that *BAT2* repression in glutamine can be alleviated in a *ure2*Δ mutant or through Gcn4-dependent transcriptional activation. Thus, when *S. cerevisiae* is grown on glutamine, VIL biosynthesis is predominant and is preferentially achieved through *BAT1*; while on VIL as the sole nitrogen source, catabolism prevails and is mainly afforded by *BAT2*.

KEYWORDS functional diversification; expression regulation; aminotransferases; amino acid metabolism; paralogous genes

GENE duplication is a key evolutionary mechanism resulting in the emergence of diversified genes, with new or specialized functions (Ohno 1970; Zhang 2003; Conant and Wolfe 2008). Phylogenomic studies have indicated that the contemporaneous occurrence of interspecies hybridization and genome duplication has driven the organization of the genome, as is currently observed in *Saccharomyces cerevisiae* (Wolfe and Shields 1997; Marcet-Houben and Gabaldón 2015). After whole genome duplication, functional normal ploidy was recovered as a result of the loss of 90% of duplicated genes (Mewes *et al.* 1997). In addition, selective retention and subfunctionalization of gene pairs derived from ancestral bifunctional genes have led to the distribution of the ancestral function(s) between the paralogous copies (DeLuna *et al.* 2001; Quezada *et al.* 2008; López *et al.* 2015). Various modes of gene diversification have been described, which include modification of the oligomeric organization, kinetic properties, subcellular relocalization of the paralogous enzymes (DeLuna *et al.* 2001; Quezada *et al.* 2008; Colón *et al.* 2011; López *et al.* 2015), and diversification of the regulatory profile of paralogous genes (DeLuna *et al.* 2001; Avendaño *et al.* 2005). In *S. cerevisiae*, analysis of the expression patterns of duplicated genes has

doi: https://doi.org/10.1534/genetics.117.300290
Manuscript received June 5, 2017; accepted for publication September 5, 2017; published Early Online September 14, 2017.
Supplemental material is available online at www.genetics.org/lookup/suppl/doi:10.1534/genetics.117.300290/-/DC1.
[1]Corresponding author: Departamento de Bioquímica y Biología Estructural, Instituto de Fisiología Celular, Universidad Nacional Autónoma de México, Circuito Escolar sn, 04510 Ciudad de México, México. E-mail: amanjarr@ifc.unam.mx

shown that transcriptional divergence occurs at a rapid rate in evolutionary time, and that differential or opposed expression among paralogous pairs could result from the acquisition of modified properties of both the *trans*-acting factors (TFs) and the *cis*-acting elements, which constitute promoter binding sites to which TFs are recruited. It is worth mentioning is the fact that it has also been proposed that modification of *cis*- and *trans*-acting elements does not by itself account for expression diversification and that additional factors, such as messenger RNA (mRNA) stability and local chromatin environment should also be considered (Makova and Li 2003; Gu *et al.* 2004, 2005; Zhang *et al.* 2004; Leach *et al.* 2007).

S. cerevisiae paralogous genes *BAT1* and *BAT2* encode Bat1 and Bat2 branched chain aminotransferases (BCATs), which catalyze the first step of the catabolism and the last step of the biosynthesis of branched chain amino acids (BCAAs), namely valine, isoleucine, and leucine (VIL) (Kispal *et al.* 1996; Eden *et al.* 2001) (Figure 1). *BAT1* and *BAT2* arose from the above-mentioned hybridization and whole genome duplication event (WGD), which occurred ~100–150 MYA (Kellis *et al.* 2004; Marcet-Houben and Gabaldón 2015). Previous work from our laboratory has shown that the ancestral-type yeasts *Kluyveromyces lactis* and *Lachancea kluyveri*, which descend from the pre-WGD ancestor (Kellis *et al.* 2004), each have a single *BAT* gene, *KlBAT1* and *LkBAT1*, respectively, encoding bifunctional enzymes which are involved in both VIL biosynthesis and catabolism (Colón *et al.* 2011; Montalvo-Arredondo *et al.* 2015). This dual function has been partitioned among the Bat1 and Bat2 paralogous proteins of *S. cerevisiae*. It has been further proposed that functional specialization occurred through Bat1 and Bat2 differential subcellular localization and *BAT1* and *BAT2* expression divergence (Colón *et al.* 2011). Earlier studies from our group have indicated that *BAT1* shows a biosynthetic expression profile: it is repressed when VIL is provided in the medium, and induced in the absence of VIL, on either primary nitrogen sources such as ammonium or glutamine or on secondary nitrogen sources such as γ-aminobutiric acid (GABA) (Colón *et al.* 2011). Furthermore, it has been shown that *BAT1*-induced expression is primarily dependent on Leu3–α-isopropylmalate (α-IPM) transcriptional activation (Sze *et al.* 1992) as opposed to *BAT2* regulation. Our group has also demonstrated that *BAT2* shows a catabolic expression pattern, which resembles a classic nitrogen catabolite repression (NCR) profile (Courchesne and Magasanik 1988; Minehart and Magasanik 1991; Blinder and Magasanik 1995; Coffman *et al.* 1995), that is downregulated in the presence of primary nitrogen sources such as glutamine, and upregulated in secondary nitrogen sources such as GABA or VIL (Colón *et al.* 2011). Accordingly, in the presence of VIL as sole nitrogen source, *BAT2* expression is induced, confirming its catabolic expression profile as opposed to the biosynthetic expression pattern displayed by *BAT1*.

Considering that *BAT1* and *BAT2* represent an interesting model to study the role of expression divergence on functional diversification, we have analyzed the mechanisms involved in *BAT1* and *BAT2* transcriptional regulation. Our results confirmed previous observations (Boer *et al.* 2005) indicating that *BAT1* expression under biosynthetic conditions is mainly achieved through Leu3–α-IPM. The nucleosome scanning assay (NuSA) showed that the Leu3 binding site is located in the nucleosome-free region (NFR) of the *BAT1* promoter, indicating that Leu3 has free accessibility to the promoter on either glutamine or VIL. The fact that *BAT1* expression is repressed (according to the biosynthetic expression profile) on VIL as the sole nitrogen source suggests that, under this condition, the lack of α-IPM could be hindering Leu3-dependent transcriptional activation. Accordingly, our results show that a Put3-dependent negative mechanism, which is elicited in a *put3*Δ mutant and suppressed in a *put3*Δ *leu3*Δ double mutant, exerts an indirect negative action, hindering the positive role of Leu3–α-IPM on *BAT1* transcription. Since α-IPM biosynthesis is inhibited in the presence of VIL (López *et al.* 2015), the existence of a VIL-insensitive α-IPM biosynthetic pathway could support α-IPM production and formation of the Leu3–α-IPM active isoform. The presented results show that in a *put3*Δ mutant, the combined action of Bat2-Leu2-Leu1 constitutes an α-IPM leucine-insensitive biosynthetic pathway. In regard to the *BAT2* expression profile, it was found that on glutamine as sole nitrogen source, *BAT2* repression is determined by the indirect negative effect of Ure2, as has been reported for other catabolic genes (Courchesne and Magasanik 1988; Minehart and Magasanik 1991; Blinder and Magasanik 1995; Coffman *et al.* 1995). In addition, the presented results uncover the existence of a negative Leu3-dependent role, which suppresses *BAT2* expression on glutamine. In a *leu3*Δ mutant, amino acid deprivation is elicited, allowing *BAT2*-induced expression through Gcn4. Furthermore, NuSA analysis indicated that *BAT2* transition from repressed (glutamine) to induced (VIL) expression is accompanied by chromatin remodeling.

Our results underscore the fact that the directly or indirectly opposed regulatory action of TFs, the location of *cis*-acting elements in *BAT1* and *BAT2* promoters, chromatin organization, and the metabolic status of the cell afford crucial pathways which have influenced the functional role of the paralogous BCATs in *S. cerevisiae*.

Materials and Methods

Growth conditions

Strains were grown on minimal medium (MM) containing salts, trace elements, and vitamins according to the formula for yeast nitrogen base (Difco, Detroit, MI). Glucose (2% w/v) was used as carbon source and Gln (7 mM), GABA (7 mM), or valine (150 mg/liter) plus leucine (100 mg/liter) plus isoleucine (30 mg/liter) were used as nitrogen sources. Uracil (20 mg/liter) and leucine (100 mg/liter) were added as auxotrophic requirements when needed. Cells were incubated at 30° with shaking (250 rpm).

In silico promoter analysis

We examined a 600-bp intergenic region upstream of the start codon of the BCAA transaminase genes of the *S. cerevisiae* genome. The 1500-bp sequences upstream of the predicted

start codon were subject to *in silico* promoter analysis (Supplemental Material, Figure S1 and Figure S2). All genomic sequences analyzed in this study were obtained from the Yeast Gene Order Browser database (Byrne and Wolfe 2005). Sequences were subject to motif scanning using the Matrix Scan program, a member of the Regulatory Sequence Analysis Tools package (Van Helden 2003; Thomas-Chollier *et al.* 2008, 2011; Turatsinze *et al.* 2008). The yeast transcription factor matrix motifs used for this analysis were downloaded from the Yeast Transcription Factor Specificity Compendium database (De Boer and Hughes 2012).

Strains

S. cerevisiae strains used in this work are described in Table 1. All *S. cerevisiae* strains are isogenic derivatives of the previously described CLA11-700 (*MAT*α *leu2*::*LEU2 ura3*) (DeLuna *et al.* 2001). The isogenic *gcn4*Δ (CLA11-708), *leu3*Δ (CLA11-709), *gln3*Δ (CLA11-710), *put3*Δ (CLA11-711), *ure2*Δ (CLA11-712), *nrg1*Δ (CLA11-713), *gat1*Δ (CLA11-714), *hap2*Δ (CLA11-715), and *mot3*Δ (CLA11-716) were obtained from strain CLA11-700 by gene replacement. A PCR-generated *kanMX4* module was prepared from plasmid pFA6a (Table S1 in File S1) following a previously described method (Longtine *et al.* 1998) using J1–J18 deoxyoligonucleotides (Table S2 in File S1). Double mutants were constructed as follows: The *kanMX4* module from CLA11-709 *leu3*::*kanMX4* was replaced by the *natMX4* cassette, which confers resistance to the antibiotic nourseothricin (Goldstein and McCusker 1999). The *natMX4* cassette used for transformation was obtained by digesting plasmid p4339 (Table S1 in File S1) with *Eco*RI. The *leu3*::*natMX4* strain (CLA11-717) was transformed following a previously described method (Ito *et al.* 1983). Double *put3*Δ *leu1*Δ (CLA11-719) and *put3*Δ *bat2*Δ (CLA11-737) mutants were prepared by transforming *put3*Δ (CLA11-711) by inserting a PCR module containing the *URA3* gene amplified from plasmid pKT175 (Sheff and Thorn 2004) in *LEU1*, or the *natMX4* module from plasmid p4339 (Table S1 in File S1) to delete *BAT2* using J19-J20 or J20A-J20B deoxyoligonucleotides, respectively (Table S2 in File S1). The double *gcn4*Δ *leu3*Δ (CLA11-720), *put3*Δ *leu3*Δ (CLA11-721) mutants were prepared by transforming the *leu3*Δ (CLA11-717) with *kanMX4* modules by replacing *GCN4* or *PUT3*, respectively, using the deoxyoligonucleotides described in Table S2 in File S1 (J1-J2 or J7-J8, respectively). The double mutant *gln3*Δ *ure2*Δ (CLA11-722) was constructed by replacing *GLN3* and *URE2* with *natMX4* and *kanMX4* modules as described above. Transformants were selected for either G418 resistance (200 mg/liter; Life Technologies), or nourseothricin resistance (100 mg/liter; Werner Bio Agents), on yeast extract, peptone, dextrose medium (YPD). Single and double mutants were PCR verified. The triple *leu4*Δ *leu9*Δ *leu1*Δ (strain CLA11-736) mutant was obtained from strain CLA11-700 by gene replacement. Three PCR modules (*kanMX4*, *natMX4*, and *URA3*) were prepared from plasmids, pFA6a, p4339, and pKT175 (Table S1 in File S1) following a previously described method (Longtine *et al.* 1998) using J20C-J20D, J20E-J20F, and J19-J20 deoxyoligonucleotides (Table S2 in File S1). The *LEU4*, *LEU9*, and *LEU1* loci were replaced by the *kanMX4*, *natMX4*, and *URA3* modules, respectively. Transformants were simultaneously selected for both G418 resistance and nourseothricin resistance on YPD as described above. Transformants resistant to nourseothricin and G418 were selected on plates with MM plus glucose without uracil. The triple mutant was PCR verified. The strain CLA11-732 (*MAT*α P_{ENO2}*LEU4* P_{ENO2}-*LEU9 leu1*::*URA3 leu2*::*LEU2*) was prepared from the isogenic strain CLA11-706 (*MAT*α *ENO2pr-LEU4 ENO2pr-LEU9 leu2*::*LEU2*) (López *et al.* 2015) by inserting a PCR module containing the *URA3* gene amplified from plasmid pKT175 (Sheff and Thorn 2004) in *LEU1* using J19-J20 deoxyoligonucleotides (Table S2 in File S1). *PUT3*-tandem affinity purification (TAP) BY4741 *ura3 leu2 his3 met5* was obtained from the TAP-tagged *Saccharomyces* strain collection.

Construction of myc-tagged strains

GCN4-myc^{13} (CLA11-723), *GLN3-myc*^{13} (CLA11-724), and *LEU3-myc*^{13} (CLA11-725) strains were tagged with the 13-myc-*kanMX4* module obtained from plasmid pFA6a-*myc*^{13}-kanMX6 (Goldstein and McCusker 1999) (Table S3 in File S1) using J21–J26 deoxyoligonucleotides (Table S3 in File S1). The *GCN4-myc*^{13}*leu3Δ* (CLA11-734) strain was prepared from the *GCN4-myc*^{13} (CLA11-723) isogenic strain, and the *LEU3* locus was replaced with the *leu3*::*natMX4* module obtained from the *leu3*::*natMX4* (CLA11-717) strain by homologous recombination, using the J26-A and J26-B deoxyoligonucleotides (Table S3 in File S1). The *LEU3-myc*^{13} *leu3*$_{box}$ (CLA11-735) strain was prepared from CLA11-730 *leu3*$_{box}$ (*MAT*α P_{BAT2} CCGCTTTCGG::CCGCTTTaaa *ura3 leu2*::*LEU2*), and *LEU3* was tagged with the 13-myc-*kanMX4* module obtained from plasmid pFA6a-*myc*^{13}-kanMX6 using J25-J26 deoxyoligonucleotides (Table S3 in File S1). Transformants were selected for G418 resistance (200 mg/liter; Life Technologies) or nourseothricin resistance (100 mg/liter; Werner Bio Agents) on YPD. Strains were PCR verified.

Northern blot analysis

Northern blot analysis was performed as previously described (Valenzuela *et al.* 1998). Total yeast RNA was extracted following the method of Struhl and Davis (1981). Cultures were grown to an OD_{600} ~0.5 in MM with glutamine or VIL as sole nitrogen sources and 2% glucose as carbon source. Aliquots of 50 ml were used to obtain total RNA. PCR-specific products for *BAT1*, *BAT2*, *ACT1*, *SCR1*, *DAL5*, *HIS4*, *LEU1*, and *LEU2* were generated from genomic DNA using J27–J50 deoxyoligonucleotides (Table S4 in File S1) and radioactively labeled by α-^{32}P dCTP with the Random Primer Labeling Kit (catalog number 300385; Agilent). These were respectively used as hybridization probes for the mRNA of *BAT1*, *BAT2*, *ACT1*, *SCR1*, *DAL5*, *HIS4*, *LEU1*, and *LEU2*. Blots were scanned using the ImageQuant 5.2 (Molecular Dynamics) program. Representative results of three experiments are presented.

NuSA

Nucleosome scanning experiments were performed by adapting a previously described method (Biddick *et al.* 2008; Infante

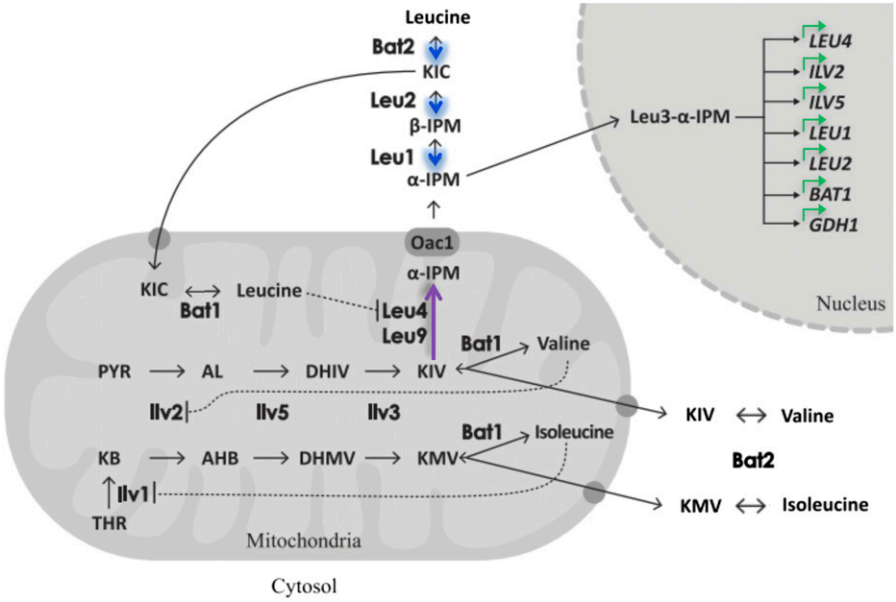

Figure 1 Diagrammatic representation of the biosynthetic pathway of BCAAs of *S. cerevisiae*. The proteins that participate in the pathway are Leu4/Leu9 (α-IPMSs, which constitute the leucine-sensitive α-IPM biosynthetic pathway), Oac1 (mitochondrial inner membrane transporter), Leu1 (isopropyl malate isomerase), Leu2 (β-IPM dehydrogenase), Bat1 (mitochondrial BCAT), Bat2 (cytoplasmic BCAT), threonine deaminase (Ilv1), acetolactate synthase (Ilv2), acetohydroxiacid reductoisomerase (Ilv5), dihydroxiacid dehydratase (Ilv3), α-ketoisocaproate (KIC), β-IPM, α-IPM, pyruvate (PYR), acetolactate (AL), α.β-dehydroxyisovalerate (DHIV), α-ketoisovalerate (KIV), α-ketobutanoate (KB), α-keto-2-hydroxybutyrate (AHB), dihydroxymetylvalerate (DHMV), α-ketomethylvalerate (KMV), threonine (THR). Dotted lines represent negative allosteric feedback loops. Filled circles represent presumed transporters. The expression of the genes (*LEU4*, *ILV2*, *ILV5*, *LEU1*, *LEU2*, *BAT1*, and *GDH1*) proceeded by an arrow are positively regulated by Leu3 (green arrow depicts transcriptional activation). The leucine-sensitive α-IPM pathway is depicted with a purple arrow, while the arrows pertaining the leucine resistant pathway are shaded in blue.

et al. 2012). Wild-type *S. cerevisiae* strain was grown in 50 ml MM with 2% glucose with 7 mM glutamine or valine (150 mg/liter) plus isoleucine (30 mg/liter) plus leucine (100 mg/liter) to an ~0.5 OD_{600}. A final formaldehyde concentration of 1% was added for 20 min at 37°, after which 125 mM glycine was supplied for 5 min at 37°. Formaldehyde-treated cells were harvested by centrifugation, washed with Tris-buffered saline, and then incubated in Buffer Z2 (1 M sorbitol, 50 mM Tris-Cl at pH 7.4, 10 mM β-mercaptoethanol) containing 2.5 mg of zymolyase 20T for 20 min at 30° on a shaker. Spheroplasts were pelleted by centrifugation at 3000 × *g*, and resuspended in 1.5 ml of NPS buffer (0.5 mM spermidine, 0.075% NP-40, 50 mM NaCl, 10 mM Tris, pH 7.4, 5 mM $MgCl_2$, 1 mM $CaCl_2$, 1 mM β-mercaptoethanol). Samples were divided in three 500-μl aliquots which were then digested with 22.5 unit of MNase (Nuclease S7 from Roche) at 50 min at 37°. Digestions were interrupted with 12 μl of stop buffer (50 mM EDTA and 1% SDS) and treated with 100 μg of proteinase K at 65° overnight. DNA was extracted twice with phenol/chloroform and precipitated with 20 μl of 5 M NaCl and an equal volume of isopropanol for 30 min at −20°. Precipitates were then resuspended in 40 μl of TE buffer and incubated with 20 μg RNase A for 1 hr at 37°. DNA digestions were performed as previously reported (Infante *et al.* 2012). Monosomal bands were cut and purified using the Wizard SV Gel Clean-Up System Kit (reference A9282; Promega, Madison, WI). DNA samples were diluted 1:30 and used for quantitative PCR (qPCR) to independently determine the relative MNase protection of *BAT1* (YHR208W) and *BAT2* (YJR148W) templates. qPCR analysis was performed using a Corbett Life Science Rotor Gene 6000 machine. SYBR Green was used as detection dye (2× KAPA SYBR FASTq Bioline and Platinum SYBR Green; Invitrogen, Carlsbad, CA). qPCR was carried out as follows: 94° for 5 min (one cycle), 94° for 15 sec, 58° for 20 sec, and 72° for 20 sec (35 cycles). The relative protection of *BAT1* and *BAT2* was calculated as a ratio considering the amplification of a region of *VCX1* with the following deoxyoligonucletide pairs: forward, 5′-TGC GTG TGC ATC CCT ACT GA-3′; and reverse, 5′-AAG TGG TCT TCC TTG CCA TGA-3′. PCR deoxyoligonucleotides are described in Tables S5 and S6 in File S1, which amplify from around −600 to +250 bp of *BAT1* or *BAT2* loci whose coordinates are given relative to the ATG +1. All presented NuSAs represent the mean values and SE of at least three independent biological replicates.

Metabolite extraction and analysis

Cell extracts were prepared from exponentially growing cultures (OD_{600} 0.3 and 0.6). Samples used for intracellular amino acid determination were treated as previously described (Quezada *et al.* 2008).

Quantitative chromatin immunoprecipitation

Formaldehyde cross-linking and immunoprecipitations were carried out by adapting a previously described procedure (Hernández *et al.* 2011). Yeast cells (200 ml of OD_{600} 0.5) were cross-linked with 1% formaldehyde for 20 min at room temperature. Afterward, 125 mM glycine was added and incubated for 5 min. Cells were then harvested and washed with PBS buffer. Pelleted cells were suspended in lysis buffer (140 mM NaCl, 1 mM EDTA, 50 mM HEPES/KOH, 1% Triton X-100, 0.1% sodium deoxycholate) with a protease inhibitor cocktail (Complete Mini, Roche). Cells were lysed with glass

Table 1 Yeast strains used in this study

Strain	Genotype	Source
CLA11-700	*S. cerevisiae MATα ura3 leu2::LEU2*	DeLuna *et al.* (2001)
BY4741 *PUT3*-TAP	*S. cerevisiae ura3 leu2 his3 met5 PUT3-TAP*	TAP collection
CLA11-706	*MATα ENO2pr-LEU4 ENO2-prLEU9 leu2::LEU2*	López *et al.* (2015)
CLA11-708 *gcn4Δ*	*MATα gcn4::kanMX4 ura3 leu2::LEU2*	This study
C1LA1-709 *leu3Δ*	*MATα leu3::kanMX4 ura3 leu2::LEU2*	This study
CLA11-710 *gln3Δ*	*MATα gln3::kanMX4 ura3 leu2::LEU2*	This study
CLA11-711 *put3Δ*	*MATα put3::kanMX4 ura3 leu2::LEU2*	This study
CLA11-712 *ure2Δ*	*MATα ure2::kanMX4 ura3 leu2::LEU2*	This study
CLA11-713 *nrg1Δ*	*MATα nrg1::kanMX4 ura3 leu2::LEU2*	This study
CLA11-714 *gat1Δ*	*MATα gat1::kanMX4 ura3 leu2::LEU2*	This study
CLA11-715 *hap2Δ*	*MATα hap2::kanMX4 ura3 leu2::LEU2*	This study
CLA11-716 *mot3Δ*	*MATα mot3::kanMX4 ura3 leu2::LEU2*	This study
CLA11-717 *leu3Δ*	*MATα leu3::natMX4 ura3 leu2::LEU2*	This study
CLA11-719 *put3Δleu1Δ*	*MATα put3::kanMX4 leu1::URA3 leu2::LEU2*	This study
CLA11-720 *gcn4Δleu3Δ*	*MATα gcn4::kanMX4 leu3::natMX4 ure3 leu2::LEU2*	This study
CLA11-721 *put3Δleu3Δ*	*MATα put3::kanMX4 leu3::natMX4 ure3 leu2::LEU2*	This study
CLA11-722 *ure2Δgln3Δ*	*MATα ure2::kanMX4 gln3::natMX4 ura3 leu2*	This study
CLA11-723 *GCN4-myc^{13}*	*MATα GCN4-myc^{13}::kanMX4 ura3 leu2::LEU2*	This study
CLA11-724 *GLN3-myc^{13}*	*MATα GLN3-myc^{13}::kanMX4 ura3 leu2::LEU2*	This study
CLA11-725 *LEU3-myc^{13}*	*MATα LEU3-myc^{13}::kanMX4 ura3 leu2::LEU2*	This study
CLA11-726 *gata$_{boxes}$*	*MATα P_{BAT1} GATAAT::GcaAAT, GATAAA::GcaAAA, GATAAT::GcaAAT, GATAAG::GcaAAG ura3 leu2::LEU2*	This study
CLA11-727 *leu3$_{box}$*	*MATα P_{BAT1} GCCGGTACCGGC::aaaGGTACCaaa ura3 leu2::LEU2*	This study
CLA11-728 *put3$_{box}$*	*MATα P_{BAT1} CGCTGGATAAGTACCG::aaaTGGATAAGTAaaa ura3 leu2::LEU2*	This study
CLA11-729 *gata$_{box}$*	*MATα P_{BAT2} GTTATC::GTTtgC ura3 leu2::LEU2*	This study
CLA11-730 *leu3$_{box}$*	*MATα P_{BAT2} CCGCTTTCGG::CCGCTTTaaa ura3 leu2::LEU2*	This study
CLA11-731 *put3$_{box}$*	*MATα P_{BAT2} CGGCGTTCTTTTTCGG::aaaCGTTCTTTTTCGG ura3 leu2::LEU2*	This study
CLA11-732	*MATα P_{ENO2}LEU4 P_{ENO2}LEU9 leu1::URA3 leu2::LEU2*	This study
CLA11-733 *leu4Δleu9Δ*	*MATα leu4::URA3 leu9::kanMX4 leu2::LEU2*	López *et al.* (2015)
CLA11-734 *GCN4-myc^{13}leu3Δ*	*MATα GCN4-myc^{13}::kanMX4 ura3 leu2::LEU2*	This study
CLA11-735 *LEU3-myc^{13}leu3$_{box}$*	*MATα P_{BAT2} CCGCTTTCGG::CCGCTTTaaa LEU3-myc^{13}::kanMX4 ura3 leu2::LEU2*	This study
CLA11-736 *leu4Δleu9Δleu1Δ*	*MATα leu4::kanMX4 leu9::natMX4 leu1::URA3 leu2::LEU2*	This study
CLA11-737 *put3Δbat2Δ*	*MATα put3::kanMX4 bat2::natMX4 ura3 leu2::LEU2*	This study

beads and collected by centrifugation. Extracts were sonicated with a Diagenode Bioruptor to produce chromatin fragments with an average size of 300 bp. Immunoprecipitation reactions were carried out with 1 mg anti-c-Myc antibody (9E11, Santa Cruz Biotechnology) and protein A beads for 3 hr, washed, suspended in TE buffer/1% SDS, and incubated overnight at 65° to reverse the formaldehyde cross-linking. Immunoprecipitates were then incubated with proteinase K (Roche), followed by phenol/chloroform/isoamyl alcohol extraction, precipitation, and suspension in 30 μl TE buffer. Dilutions of input DNA (1:100) and immunoprecipitated DNA (1:2) were analyzed by qPCR. Real-time PCR-based DNA amplification was performed using specific primers that were initially screened for dimer absence or cross-hybridization. Only primer pairs with similar amplification efficiencies were used (Table S7 in File S1). Quantitative chromatin immunoprecipitation (qChIP) analysis was performed using a Corbett Life Science Rotor Gene 6000 machine. The fold difference between immunoprecipitated material (IP) and total input sample for each qPCR-amplified region was calculated following the formula IP/input = ($2^{\text{InputCt} - \text{IPCt}}$) (Litt *et al.* 2001). The results presented represent the mean values and SE of at least three independent, cross-linked samples with each sample being immunoprecipitated twice with the antibody.

Construction of site-specific DNA mutations

Mutants altered in *cis*-acting elements were constructed by transforming wild-type strain CLA11-700 with a 3.2-kb fragment obtained by PCR amplification of the pCORE plasmid harboring the *kanMX4* and *URA3 CORE* modules (Storci and Resnick 2003). Transformations were carried out following the previously described protocol (Ito *et al.* 1983). Colonies were isolated on YPD-G418 (200 mg/liter). Correct insertion was verified by PCR amplification. The transformants were retransformed with integrative recombinant oligonucleotides harboring mutagenized modules (Figure S3 and Table S8 in File S1). The strains generated were CLA11-726 (*GATA* boxes at positions −424, −415, −374, and −324 in the *BAT1* promoter, from G**AT**AAT, G**AT**AAA, G**AT**AAT, and G**AT**AAG to G**ca**AAT, G**ca**AAA, G**ca**TAAT, and G**ca**AAG), CLA11-727 (*LEU3* binding site at positions −150 and −141 in the *BAT1* promoter, from **GCC**GGTACC**GGC** to **aaa**GGTACC**aaa**), CLA11-728 (*PUT3* binding site at positions −163 and −150 in the *BAT1* promoter, from **CGC**TGGATAAGTA**CCG** to **aaa**TGGATAAGTA**aaa**), CLA11-729 (*GATA* box at position −282 in the *BAT2* promoter, from GTT**AT**C to GTT**tg**C), CLA11-730 (*LEU3* binding site at position −327 in the *BAT2* promoter, from **CCG**CTTT**CGG** to **CCG**CTTT**aaa**), and CLA11-731 (*PUT3* binding site at position −347 in the *BAT2*

promoter, from **CGG**CGTTCTTTTTCGG to **aaa**CGTTCTTTTTCGG). After transformation, 5-FOA-resistant colonies were analyzed by PCR. The correct insertion was confirmed by sequencing with an Applied Biosystems (Foster City, CA) 3100 Genetic Analyzer.

Data availability

The 32 strains listed in Table 1 and plasmids described in Table S1 in File S1 are available upon request. Sequences performed to confirm *cis*-element mutants are described in Figure S3. Data concerning sequence analysis of TF binding sites and mutant phenotypes are presented in Figure S1, Figure S2, Figure S4, Figure S5, and Figure S6.

Results

Identification of the presumed cis-acting elements located on the BAT1 and BAT2 promoters and assessment of their accessibility by NuSA

To identify the presumed *cis*-acting factors that could influence *BAT1* and *BAT2* expression, DNA sequence of both promoter regions was analyzed with the pertinent bioinformatic tools (*Materials and Methods*). The occupancy of the *cis*-acting sequences was assessed by analyzing the chromatin organization profile determined by NuSA. As a positive control, gene expression was monitored by Northern blot analysis in samples obtained from the same cultures, from which chromatin organization assays of *BAT1* and *BAT2* promoters were performed (OD_{600} 0.5), as described in *Materials and Methods*. As expected, expression analysis confirmed the previously reported *BAT1* biosynthetic profile (VIL repressed) and *BAT2* catabolic profile (VIL induced), since expression is only observed in the presence of VIL (Colón *et al.* 2011) (Figure 2A).

NuSAs were carried out to determine nucleosome positioning and occupancy of presumed *cis*-acting elements across the *BAT1* and *BAT2* promoters in wild-type cells grown on glutamine or VIL as sole nitrogen sources. qPCR was carried out with 30 or 29 primer pairs, respectively, for *BAT1* or *BAT2* (Tables S5 and S6 in File S1) to independently amplify overlapping regions of both promoters (Figure 2, B and C). Peaks of relative protection indicated that in either glutamine or VIL, four nucleosomes were similarly positioned around the *BAT1* transcriptional starting point (−2, −1, +1, and +2) (Figure 2B). Nucleosome −1 and +1 constitute the border of the 150-bp, MNase-sensitive NFR, which spans from around −200 to −100 with respect to the *BAT1* +1 ATG (Figure 2B). This indicates that *BAT1* differential expression on glutamine or VIL does not require chromatin remodeling. The presumed *cis*-acting elements present in the *BAT1* and *BAT2* promoters were identified through a comparative *in silico* analysis of their location (Figure 3, A and B). For *BAT1*, the *HAP2*, *MOT3*, *GCN4*, and *LEU3* presumed binding sites were located within the NFR (Figure 2B and Figure 3A). NuSA analysis of the *BAT2* promoter revealed that, in glutamine, at least four nucleosomes designated −2, −1, +1, and +2 were firmly positioned (Figure 2C), indicating occupation of the $TATA_{BOX}$ in accordance with glutamine-repressed expression pattern (Figure 2A). The NuSA profile observed on VIL for the *BAT2* promoter showed that the region from −150 to −50, harboring the $TATA_{BOX}$, was nucleosome free, suggesting higher expression as compared to that observed on glutamine. It was also found that *NRG*, *HAP2*, *LEU3*, and *PUT3* sites would be nucleosome protected in either glutamine or VIL, whereas the *GLN3-GAT1* *cis*-acting elements would be exposed under both conditions and *GCN4* only uncovered on VIL (Figure 2C and Figure 3B). It can thus be proposed that *BAT2* differential regulation on glutamine or VIL could be affected by chromatin remodeling.

Gln3, Gcn4, Leu3, and Put3 TFs, determine BAT1 and/or BAT2 expression profile

To analyze whether the *trans*-acting elements that should bind the above-described *cis*-acting factors had a role in *BAT1* and *BAT2* expression, deletion mutants were constructed in the corresponding coding genes: *GLN3-GAT1* (Blinder and Magasanik 1995), *NRG1* (Zhou and Winston 2001), *LEU3* (Friden and Schimmel 1988; Kohlhaw 2003), *PUT3* (Siddiqui and Brandriss 1989), *MOT3* (Martínez-Montañés *et al.* 2013), *GCN4* (Hinnebusch and Fink 1983; Hinnebusch 1984), and *HAP2* (Guarente *et al.* 1984). As shown in Figure S4, *nrg1*Δ, *gat1*Δ, *hap2*Δ, and *mot3*Δ mutant strains showed *BAT1* and *BAT2* wild-type expression profiles; indicating that, under the conditions tested, the encoded regulators played no role in *BAT1* or *BAT2* transcriptional regulation. Northern blot analysis was carried out on samples obtained from cultures in which Gln, GABA, or VIL were used as sole nitrogen sources, confirming the previously observed effect of both the quality of the nitrogen source and the peculiar effect of VIL on *BAT1* and *BAT2* expression (Colón *et al.* 2011). As opposed to that found for *NRG1*, *GAT1*, *HAP2*, and *MOT3* mutants; *gcn4*Δ, *leu3*Δ, *gln3*Δ, and *put3*Δ displayed a distinct phenotype when Northern blot analysis was carried out on total RNA samples (Figure 4A and Figure 5A).

Role of Gcn4 and Gln3 TFs on BAT1 and/or BAT2 expression profile

When total RNA was prepared from glutamine-grown cells (biosynthetic conditions), it was found that Gcn4 and Gln3 displayed a positive effect on *BAT1* transcriptional activation, showing no adverse effects on that of *BAT2* (Figure 4A). On VIL-grown (catabolic conditions) yeasts, Gln3 played a positive role on *BAT1* expression but showed no adverse effects on that of *BAT2*, while Gcn4 showed no effect on either *BAT1* or *BAT2* expression on this condition (Figure 4A).

To analyze whether Gln3 and Gcn4 were acting by direct binding on *BAT1* and *BAT2* promoters, qChIP experiments were carried out as described in *Materials and Methods*. To this end, Gcn4-*myc*^{13} and Gln3-*myc*^{13} derivatives were constructed (*Materials and Methods*) and their capacity to sustain wild-type transcriptional regulation was assessed (Figure S5). Amplification of three different regions of *BAT1* (Figure 4B, R1–R3) or *BAT2* (Figure 4B, R1′–R3′) promoters was analyzed by qChIP analysis. Gcn4-*myc*^{13} readily bound the *BAT1* promoter, but not the

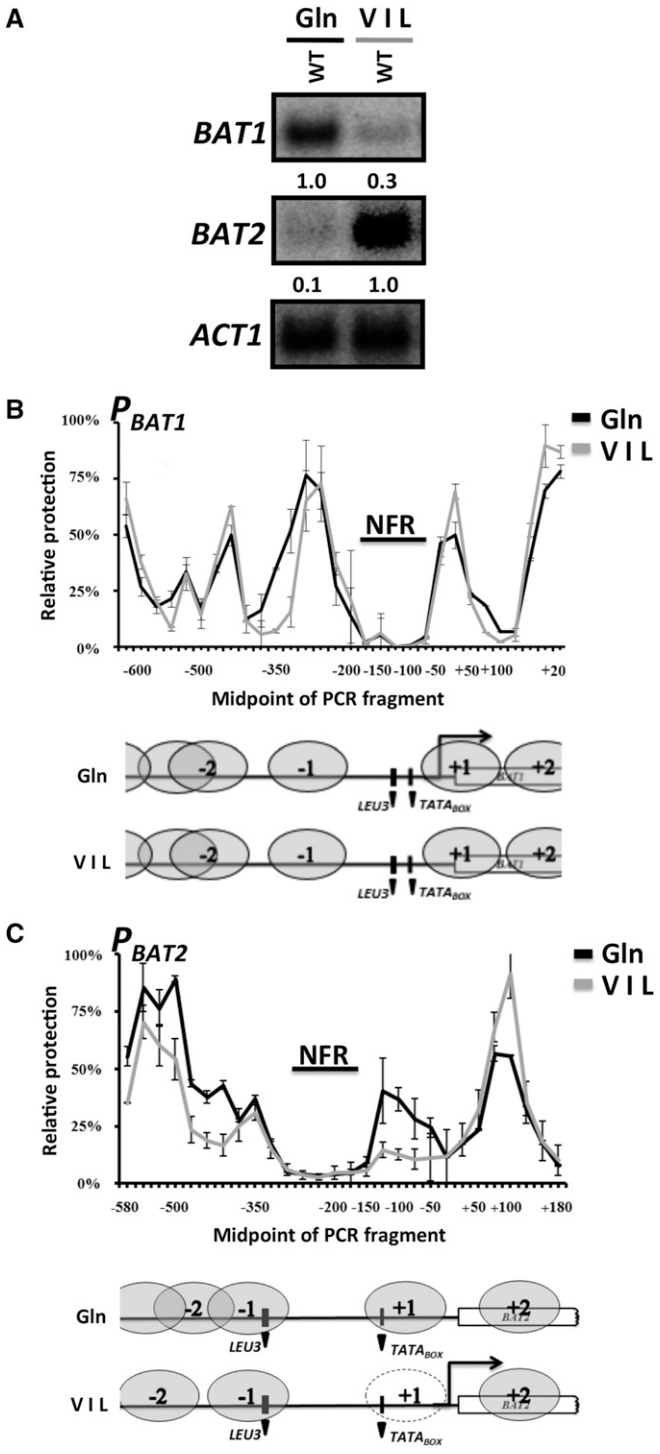

Figure 2 Northern blot analysis and NuSA indicate that opposed *BAT1* and *BAT2* transcriptional regulation is partially determined by chromatin organization. (A) Northern blot analysis was carried out on total RNA obtained from *S. cerevisiae* wild-type (WT) strain CLA11-700. Yeast cultures were grown on 2% glucose with either glutamine (7 mM) or valine (150 mg/liter) plus isoleucine (30 mg/liter) plus leucine (100 mg/liter) (VIL) as sole nitrogen sources, to an OD_{600} 0.5. Filters were sequentially probed with *BAT1*- or *BAT2*-specific PCR products as described in *Materials and Methods*. A 1500-bp *ACT1* DNA PCR fragment was used as loading control, numbers represent means of *BAT1*/*BAT2* signals normalized to those of *ACT1*. SD was calculated and corresponds to ±0.12. (B and C) For NuSA, mononucleosomes were prepared from wild-type strain cultures grown on Gln (black line) or VIL (gray line), as described in *Materials and Methods*. NuSA examined nucleosome occupancy at the *BAT1* and *BAT2* locus, including the 5′ ±600 bp of the intergenic region and the 3′ ±200 bp of *BAT1* (B) and *BAT2* (C). MNase-treated chromatin and purified DNA samples and mononucleosome-sized (140–160) fragments were prepared as described in *Materials and Methods*. The resulting material was analyzed with a set of overlapping primer pairs covering the *BAT1* and *BAT2* locus (Tables S5 and S6 in File S1). Relative *BAT1* and *BAT2* MNase protection was calculated as the ratio of template present in MNase-digested DNA over the amount of MNase protection observed for the *VCX1* locus, which was used as control. Data are presented as the average of three independent experiments along with the SEM. The diagram of the *BAT1* or *BAT2* promoters was extrapolated from the MNase protection data and depicts nucleosome positioning. Gray ovals indicate firmly positioned nucleosomes, while white ovals with dotted border depict relative occupancy. Black arrows indicate activation of transcription. Black boxes correspond to the *LEU3* binding site and $TATA_{BOX}$.

BAT2 promoter (Figure 4C); this is in agreement with the *gcn4*Δ mutant expression analysis, which showed that Gcn4 did not regulate *BAT2* expression (Figure 4A). It could also be considered that Gcn4 has a weak binding site on the *BAT2* promoter since, as will be shown further on, increased Gcn4 concentration evoked in a *leu3*Δ mutant allows the binding of Gcn4-*myc*^{13} to the *BAT2* promoter on glutamine (Figure 7B). As positive control, binding of Gcn4-*myc*^{13} to *HIS4* was monitored. It was observed that although Gcn4-*myc*^{13} clearly bound the *HIS4* promoter on samples prepared from glutamine- and GABA-grown cultures, binding on VIL-obtained samples was scarce as compared to that found on either glutamine or GABA. It has been shown that Gcn4 concentration is tightly regulated through the combined action of a complex translational control mechanism, which induces Gcn4 synthesis in starved cells, and a phosphorylation and ubiquitylation pathway that mediates its rapid degradation by the proteasome (Hinnebusch 2005; Rawal *et al.* 2014). However, Gcn4 abundance has not been determined in cultures grown on VIL as sole nitrogen source, and there is no evidence suggesting the preferential degradation of Gcn4 under this condition. Thus, the observation reported here could be attributed to the fact that, in the presence of leucine, target of rapamycin complex 1 (TORC1)-dependent m*GCN4* translation is impaired (Valenzuela *et al.* 2001; Kingsbury *et al.* 2015). However, our results indicate that Gcn4-*myc*^{13} is bound to *BAT1* and *HIS4* promoters on glutamine and GABA, confirming that *BAT1* is a direct Gcn4 target.

As expected, Gln3-*myc*^{13} bound the *BAT2* promoter in the presence of VIL or GABA secondary nonrepressive nitrogen sources, but not on glutamine, which is a primary repressive nitrogen source (Figure 4D) (Courchesne and Magasanik 1988); in agreement with the observed *BAT2* expression in a *gln3*Δ mutant (Figure 4A). Gln3 did not bind the *BAT1* promoter under any of the conditions tested, although it showed a positive regulatory input on *BAT1* expression on glutamine and VIL (Figure 4, A and D). As this effect is rather mild and Gln3 cannot be detected at the *BAT1* promoter through qChIP analysis, the observed deregulation is most

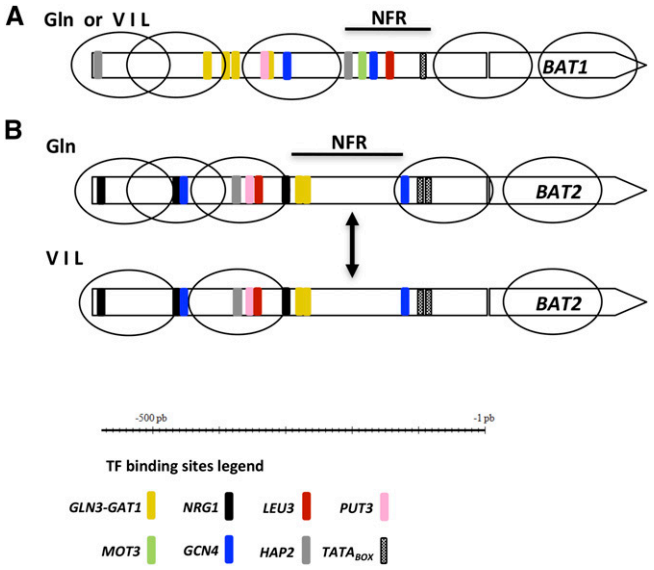

Figure 3 *BAT1* and *BAT2* promoters contain predicted *HAP2*, *GLN3-GAT1*, *GCN4*, *LEU3*, and *PUT3* binding sites. In addition to *HAP2*, *GLN3-GAT1*, *GCN4*, *LEU3*, and *PUT3*; *BAT1* harbors a *MOT3* binding site (A) and *BAT2* an *NRG1* binding sequence (B). TF binding sites are indicated as vertical color-coded rectangles, as shown in the bottom part of the figure. Ovals indicate fixed positioned nucleosomes for each analyzed promoter under Gln or VIL conditions. Double headed arrow points to either closed (Gln) or open (VIL) chromatin structure in the *BAT2* promoter region.

likely to be afforded by an indirect effect. However, to further analyze whether Gln3 acted through its direct action on the promoters, we used the "*delitto perfetto*" strategy to complement our results with *cis*-acting, site-specific mutations on Gln3 consensus and/or conserved elements in *BAT1* and *BAT2* promoters. A mutation of the presumed Gln3 consensus binding site (GATAAG) (Bysani *et al.* 1991) located at the *BAT2* promoter (*GLN3-GAT1*) resulted in decreased *BAT2* expression (Figure 4F). For *BAT1*, a simultaneous *cis*-mutation in each one of a cluster of four presumed *GLN3-GAT1* binding sites did not affect expression (Figure 4E), confirming the observation that although *BAT1* expression on glutamine and VIL is partially activated through Gln3 (Figure 4A), the mechanism does not involve direct Gln3–promoter interaction. Consequently, the positive Gln3-dependent *BAT1* effect is indirect, while the positive *BAT2* regulation through Gln3 is direct.

Put3 and Leu3 TFs play a crucial role in the BAT1 and BAT2 regulatory subfunctionalization that determines the opposed BAT1/BAT2 expression profile

To analyze the role of Put3 and Leu3 on *BAT1* and *BAT2* expression, total RNA was prepared from glutamine-grown cells (biosynthetic conditions). It was found that, as was previously observed (Boer *et al.* 2005), *BAT1* expression activation was achieved through Leu3 (Figure 5A). However, a previously unidentified negative role for Leu3 on *BAT2* expression was detected (Figure 5A), indicating that Leu3 played a role in glutamine-dependent, *BAT2*-repressed expression and consequently that Leu3 had opposing effects on the expression of *BAT1* and *BAT2*. Under this condition, Put3 did not play a role on the expression profiles of either *BAT1* or *BAT2* (Figure 5A).

Northern blot analysis, which was carried out on total RNA prepared from cells grown on VIL as the sole nitrogen source, showed that *BAT1* expression was repressed. However, in a *put3*Δ mutant, expression was fourfold derepressed as compared to that observed in a wild-type *PUT3* strain; indicating that this modulator played a negative role on *BAT1* transcriptional activation in media supplemented with VIL as the sole nitrogen source (Figure 5A). Contrastingly, *BAT2* expression was activated by Put3 (Figure 5A), indicating that Put3 exerted opposing effects on transcriptional activation of *BAT1* and *BAT2* on VIL-grown yeast. Under this condition, Leu3 only played a positive role on *BAT1* expression, and no role on that of *BAT2*.

To analyze whether Leu3 was acting by direct binding on *BAT1* and *BAT2* promoters, qChIP experiments were carried out as described in *Materials and Methods*. To this end, Leu3-*myc*^{13} derivatives were constructed (*Materials and Methods*) and the Put3-TAP mutant strain was obtained from the *S. cerevisiae* collection (Table 1). The capacity to sustain wild-type transcriptional regulation by the *myc*^{13} or TAP-tagged derivatives was confirmed for both Leu3-*myc*^{13} and Put3-TAP (Figure S5). As presented for Gln3 and Gcn4 binding assays, three different regions of the *BAT1* (Figure 5B, R1–R3) or *BAT2* (Figure 5B, R1′–R3′) promoters were selected to analyze Put3 and Leu3 binding through qChIP analysis. Put3-TAP was found to bind *BAT2* (Figure 5C), indicating that the observed *BAT2* transcriptional activation was dependent on the direct action of Put3 on the *BAT2* promoter. However, Put3 did not bind the *BAT1* promoter (Figure 5C), indicating that the negative role exerted by this TF was indirect. As positive control, the binding of Put3 to the *PUT1* promoter was monitored (Siddiqui and Brandriss 1989). Binding to the *GRS1* promoter was used as negative control. Leu3 was bound to both *BAT1* and *BAT2* promoters in either nitrogen repressive or nonrepressing conditions (Figure 5D). As positive control, the binding of Leu3 to *ILV5* (Friden and Schimmel 1988) was monitored and *GRS1* was used as negative control.

To further analyze whether TFs acted through direct action on the promoters, we used the *delitto perfetto* strategy to obtain mutants affected in *cis*-acting, specific consensus and/or conserved sequences in *BAT1* and *BAT2* promoters. Accordingly, the mutation of the *LEU3 cis*-acting element present in the *BAT1* promoter displayed an identical phenotype to that of the *leu3*Δ mutant, decreasing *BAT1* expression on glutamine and VIL (Figure 5, A and E). Conversely, for *BAT2*, the mutation on the *LEU3 cis*-acting element did not result in derepressed expression on glutamine as that found in the *leu3*Δ mutant, suggesting an indirect effect (Figure 5, A and F). Mutation of the presumed *PUT3 cis*-acting element present in *BAT1* did not result in derepression on VIL, indicating an indirect effect (Figure 5, A and E), in agreement with the fact that Put3 did not bind the *BAT1* promoter. A

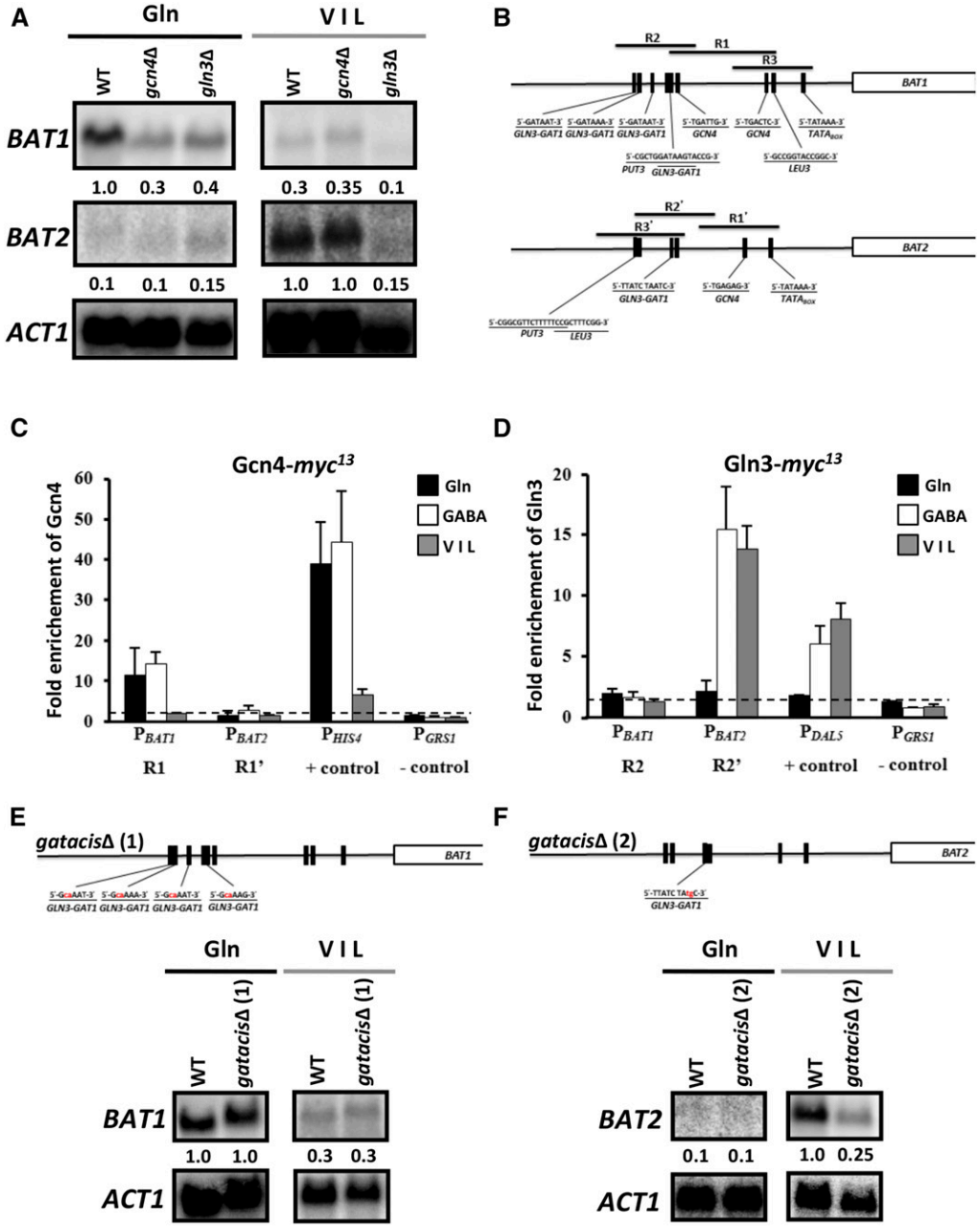

Figure 4 Role of Gcn4 and Gln3 in *BAT1* or *BAT2* expression. (A) Northern blot analysis was carried out on total RNA obtained from the wild-type (WT) strain and its isogenic *gcn4*Δ and *gln3*Δ derivatives (Table 1). Strains were grown to OD_{600} 0.5 on MM 2% glucose with either glutamine (7 mM) or valine (150 mg/liter) plus isoleucine (30 mg/liter) plus leucine (100 mg/liter) (VIL) as sole nitrogen sources. Filters were sequentially probed with *BAT1* and *BAT2* PCR products described in *Materials and Methods*. A 1500-bp *ACT1* PCR fragment was used as loading control. Numbers represent means of *BAT1*/*BAT2* signals normalized to those of *ACT1*, and the resulting ratios in the mutants normalized to those in the WT under derepressing conditions for each gene. SD was found to be ±0.10–0.12. (B) *BAT1* and *BAT2* promoter regions used to carry out qChIP assays. The three regions which were amplified for each promoter after qChIP assays (R1–R3 for *BAT1* promoter and R1′–R3′ for *BAT2* promoter) are depicted. (C and D) qChIP assays were performed using anti-Myc antibody (9E11, Santa Cruz Biotechnology) on WT strains containing *myc*^{13} epitope-tagged *GCN4-myc*^{13} and *GLN3-myc*^{13} (Table 1). Strains were grown on MM with 2% glucose and either glutamine (7 mM; solid bars), GABA (7 mM; open bars), or valine (150 mg/liter) plus isoleucine (30 mg/liter) plus leucine (100 mg/liter) (VIL; shaded bars) as sole nitrogen sources to an OD_{600} 0.5. Gcn4 (C) and Gln3 (D) binding was analyzed by qChIP, as described in *Materials and Methods*. IP/input ratios were normalized with the *GRS1* promoter as negative control (glycyl-tRNA synthase), and *HIS4* and *DAL5* promoters were respectively used as positive controls. Data are presented as the average of three independent experiments along with the SEM. (E and F) Schematic representation of *cis*-acting elements (*GLN3-GAT1*) present in *BAT1* and *BAT2* promoters, and the sequence mutations which were prepared, as described in *Materials and Methods*. Northern blot analysis was carried out on total RNA obtained from each mutant. Meaning of numbers is as described previously in this figure (see A). Strains were grown on Gln (solid line) or adding VIL (shaded line) as described previously in this figure (see A).

similar *cis*-acting mutation for the *BAT2* promoter resulted in decreased transcriptional activation, generating a phenotype equivalent to that found in a *put3*Δ mutant (Figure 5, A and F), which is in agreement with the fact that Put3 bound the *BAT2* promoter. It can thus be concluded that the negative regulation of *BAT1* and *BAT2* provided by the action of Put3 or Leu3, respectively, is indirect; while the positive regulation of *BAT1* and *BAT2* determined by Leu3 and Put3, respectively, is direct.

Under biosynthetic conditions (glutamine) Leu3 activates BAT1 expression while that of BAT2 is hindered through the negative and indirect action of Leu3 and Ure2 transcriptional regulation

The above results pose an interesting paradox in regard to the role of Leu3 on transcriptional regulation, because we show that in the presence of glutamine as nitrogen source Leu3 can either activate or repress gene expression (Figure 5A). These

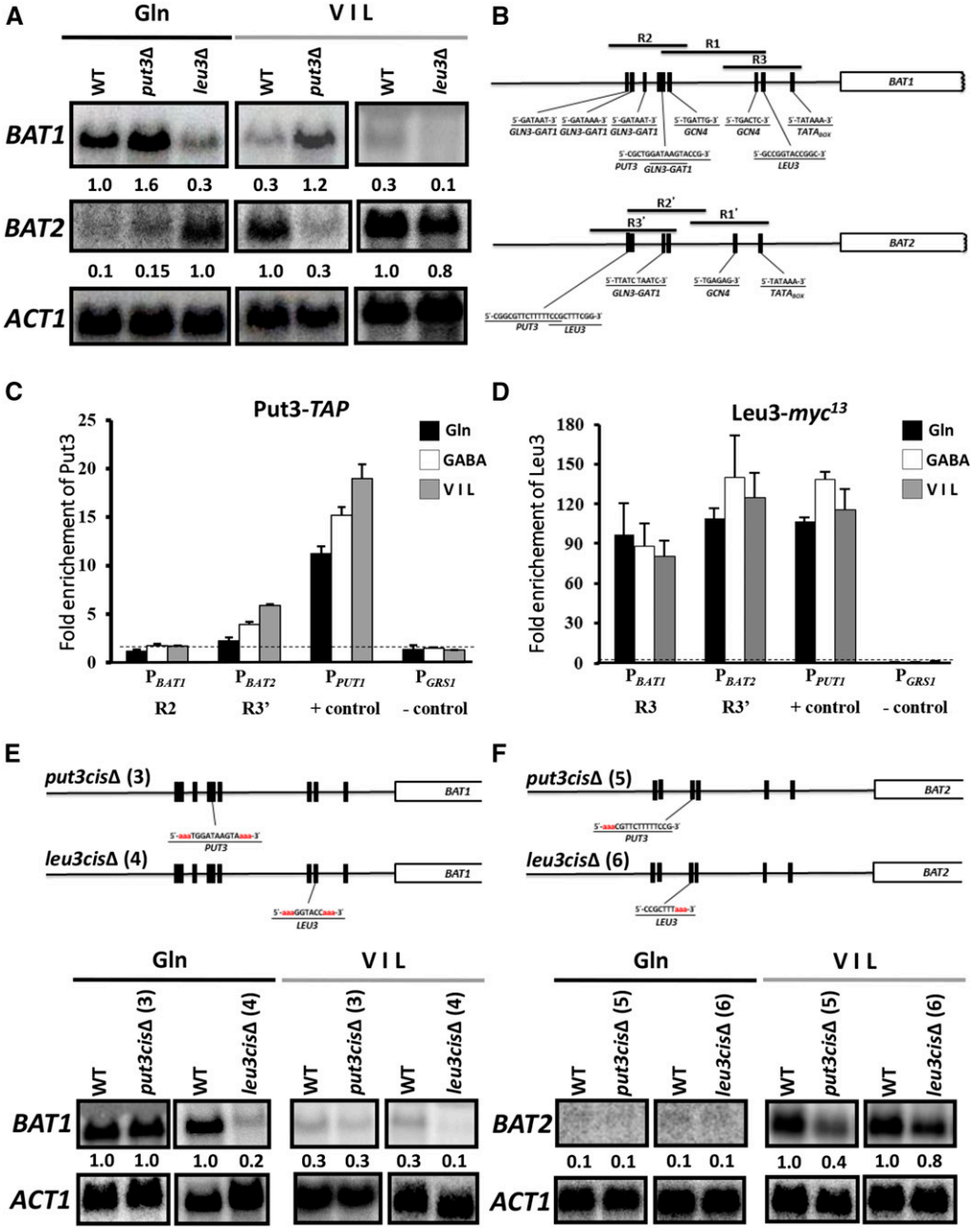

Figure 5 Put3 and Leu3 oppositely regulate *BAT1* and *BAT2* expression. (A) Northern blot analysis was carried out on total RNA obtained from the wild-type (WT) strain and its isogenic *put3*Δ and *leu3*Δ derivatives (Table 1). Strains were grown to OD_{600} 0.5 on MM with 2% glucose with either glutamine (7 mM) or valine (150 mg/liter) plus isoleucine (30 mg/liter) plus leucine (100 mg/liter) (VIL) as sole nitrogen sources. Filters were sequentially probed with *BAT1* and *BAT2* PCR products described in *Materials and Methods*. Numbers represent means of *BAT1*/*BAT2* signals normalized to those of *ACT1*, and the resulting ratios in the mutants normalized to those in the WT under derepressing conditions for each gene. SD was found to be ±0.10–0.12. A 1500-bp *ACT1* PCR fragment was used as loading control. (B) *BAT1* and *BAT2* promoter regions used to carry out qChIP assays. The three regions which were amplified for each promoter after qChIP assays (R1–R3 for *BAT1* promoter and R1′–R3′ for *BAT2* promoter) are depicted. (C and D) qChIP assays were performed using anti-Myc antibody (9E11, Santa Cruz Biotechnology) on WT strains containing myc^{13} epitope-tagged *LEU3*-myc^{13} (Table 1). For Put3 qChIP, the *PUT3*-TAP mutant from the *Saccharomyces* yeast collection was used (Table 1). Strains were grown on MM with 2% glucose and either glutamine (7 mM; solid bars), GABA (7 mM; open bars) or valine (150 mg/liter) plus isoleucine (30 mg/liter) plus leucine (100 mg/liter) (VIL; shaded bars) as sole nitrogen sources to an OD_{600} 0.5. Put3 (C) and Leu3 (D) binding was analyzed by qChIP, as described in *Materials and Methods*. IP/input ratios were normalized with the *GRS1* promoter as negative control, and *PUT1* and *ILV5* promoters were respectively used as positive controls. Data are presented as the average of three independent experiments along with the SEM. (E and F) Schematic representation of *cis*-acting elements (*PUT3* or *LEU3*) present in *BAT1* and *BAT2* promoters and the sequence mutations which were prepared, as described in *Materials and Methods*. Northern blot analysis was carried out on total RNA obtained from each mutant as described previously. Meaning of numbers is as that described in (A). SD was found to be ±0.10–0.12. Strains were grown on Gln (solid line) or adding VIL (shaded line) as described previously in this figure (see A).

results apparently contradict the proposed mode of action for Leu3 as a transcriptional regulator (Sze *et al.* 1992). The suggested model considers that in a given physiological condition, the intracellular α-IPM concentration should either allow the constitution of the Leu3 dimer, which would act as negative regulator, preventing induction; or the Leu3–α-IPM dimer activator complex, which would determine induction of target genes. However, our results show that on glutamine as sole nitrogen source, Leu3 is able to support opposite expression responses: *BAT1* induction and *BAT2* repression (Figure 5A). To further analyze this matter, we constructed a double mutant in which the two genes (*LEU4* and *LEU9*) encoding α-IPM synthase (α-IPMS) were expressed from the *ENO2* promoter, resulting in α-IPM overproduction (López *et al.* 2015). Furthermore, to avoid α-IPM catabolism to β-isopropylmalate (β-IPM), the *LEU1* gene, which encodes the sole enzyme performing this function in *S. cerevisiae*, was deleted in the P_{ENO2}*LEU4* P_{ENO2}*LEU9* mutant. The generated

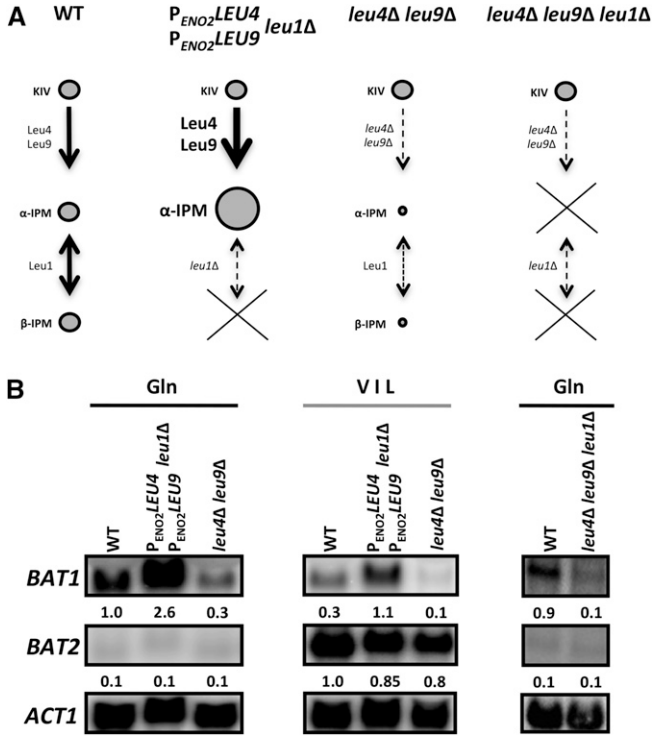

Figure 6 Leu3 determines *BAT2* expression through an α-IPM-independent mechanism. (A) Diagrammatic representation of the effect of P_{ENO2}*LEU4* P_{ENO2}*LEU9 leu1*Δ, a *leu4*Δ *leu9*Δ double mutant, and a *leu4*Δ *leu9*Δ *leu1*Δ triple mutant on α-IPM biosynthesis. (B) Northern blot analysis was carried out on total RNA samples obtained from wild-type (WT) strain and its isogenic derivatives P_{ENO2}*LEU4* P_{ENO2}*9 leu1*Δ triple mutant, *leu4*Δ *leu9*Δ double mutant, and a *leu4*Δ *leu9*Δ *leu1*Δ triple mutant (Table 1). Strains were grown to OD_{600} 0.5 on MM with 2% glucose with either glutamine (7 mM) or valine (150 mg/liter) plus isoleucine (30 mg/liter) plus leucine (100 mg/liter) (VIL) as sole nitrogen sources. Filters were sequentially probed with *BAT1* and *BAT2* PCR products described in *Materials and Methods*. A 1500-bp *ACT1* PCR fragment was used as loading control. Numbers represent means of *BAT1*/*BAT2* signals normalized to those of *ACT1*, and the resulting ratios in the mutants normalized to those in the WT under derepressing conditions for each gene. SD was found to be ±0.10–0.12.

strain P_{ENO2}*LEU4* P_{ENO2}*LEU9 leu1*Δ should feature increased α-IPM biosynthesis and null catabolism. A second mutant was constructed harboring *leu4*Δ and *leu9*Δ deletions, thus constituting a leucine auxotroph unable to synthesize α-IPM (Figure 6A), and the triple mutant *leu4*Δ *leu9*Δ *leu1*Δ, which would not be able to synthesize α-IPM through the leucine-sensitive pathway nor through the Bat2-Leu2-Leu1 leucine-resistant pathway. *BAT1* and *BAT2* expression was analyzed in these engineered strains (Figure 6B). *BAT1* expression was increased in the P_{ENO2}*LEU4* P_{ENO2}*LEU9 leu1*Δ triple mutant, as compared to that found in the wild-type strain, when grown on glutamine. The most important observation was that, in this triple mutant, *BAT1* was overexpressed even in the presence of VIL (Figure 6B), circumventing α-IPMS leucine sensitivity. As expected for a gene whose transcriptional activation is dependent on Leu3–α-IPM, increased α-IPM biosynthesis enhanced its transcriptional activation, overcoming VIL-mediated repression due to inhibition of α-IPM biosynthesis and the consequent lack of Leu3–α-IPM. The fact that, in a *leu4*Δ *leu9*Δ double mutant and *leu4*Δ *leu9*Δ *leu1*Δ triple mutant unable to synthesize α-IPM, *BAT1* expression was prevented (Figure 6B) further confirmed that the *BAT1* expression determined by Leu3 is α-IPM dependent. Conversely, *BAT2* expression was very low on glutamine in the wild-type, P_{ENO2}*LEU4* P_{ENO2}*LEU9 leu1*Δ-overexpressing, *leu4*Δ *leu9*Δ, and *leu4*Δ *leu9*Δ *leu1*Δ triple mutant strains. In VIL, *BAT2* expression was similarly induced in the α-IPM overproducing strain and in the null mutant affected in α-IPM biosynthesis. These results indicate that Leu3-dependent *BAT2* transcriptional regulation does not follow the canonical model proposed for the action of Leu3 as a transcriptional modulator (Sze *et al.* 1992) since *BAT2* expression on glutamine or VIL does not respond to increased or null levels of α-IPM. These results suggest that for *BAT1*, Leu3–α-IPM abundance directly determines induced expression; while for *BAT2*, Leu3-dependent transcriptional modulation could be indirect, eliciting the action of a positive regulator whose function is only evident in a *leu3*Δ null mutant. This proposition is supported by the fact that, as presented above, although Leu3 can bind both *BAT1* and *BAT2* promoters (Figure 5D), a *leu3*Δ *cis*-mutant in the *BAT2* promoter does not mimic the phenotype of a *leu3*Δ mutant and *BAT2* expression is not derepressed on glutamine (Figure 5F). Furthermore, we performed a qChIP assay using anti-Myc antibody (described in *Materials and Methods*) on extracts prepared from cultures of the CLA11-735 *LEU3-myc*^{13} *leu3*$_{box}$ strain. As expected, no Leu3-*myc*^{13} immunoprecipitation was observed, confirming the indirect action of Leu3 on *BAT2* expression (Figure 7A).

To analyze the presumed indirect role of Leu3 on *BAT2* glutamine-dependent repression, the *gcn4*Δ *leu3*Δ mutant was constructed as described in *Materials and Methods*. Northern blot analysis of *BAT2* expression on total RNA samples prepared from cells grown on glutamine as the sole nitrogen source showed that Leu3-dependent *BAT2* derepression in a *leu3*Δ mutant was not observed in a double mutant *gcn4*Δ *leu3*Δ (Figure 7C). Thus, the Leu3-dependent *BAT2* "repression" pattern was the result of the lack of *GCN4* expression, whose action is elicited in a *leu3*Δ mutant. Considering that Leu3–α-IPM positively regulates several biosynthetic genes such as *GDH1* (Hu *et al.* 1995), *BAT1*, *LEU1*, *LEU2*, *LEU4*, and *ILV5* (Boer *et al.* 2005); in a *leu3*Δ mutant, an amino acid deprivation could be evoked. In fact, as Table 2 shows, valine, leucine, glutamic acid, alanine, and histidine pools are decreased in a *leu3*Δ mutant on glutamine as the sole nitrogen source during the early exponential growth phase (OD_{600} 0.3), as compared with those observed in a wild-type strain. At exponential phase (OD_{600} 0.6), *leu3*Δ amino acid pools recover wild-type concentrations. As shown in Figure 7C, *HIS4* expression is increased in *leu3*Δ, but not in *gcn4*Δ *leu3*Δ. It can be thus concluded that Leu3-dependent *BAT2* expression on glutamine in a *leu3*Δ mutant is triggered through *GCN4*-dependent transcriptional activation, due to increased biosynthesis of Gcn4 provoked by amino acid

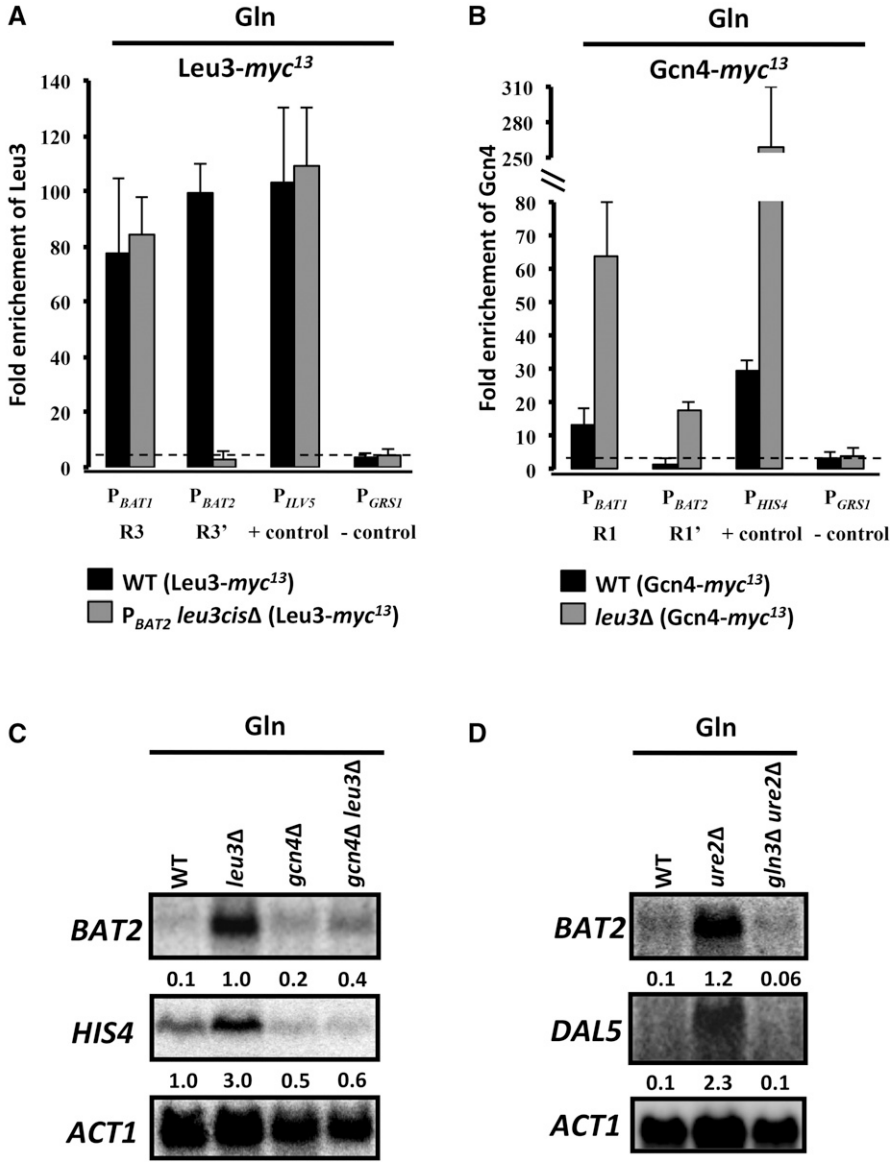

Figure 7 *BAT2* expression is indirectly determined by Leu3 and Ure2. (A and B) qChIP assays were performed using anti-Myc antibody (9E11, Santa Cruz Biotechnology) on wild-type (WT) strains containing *myc*^{13} epitope-tagged *LEU3-myc*^{13}, *LEU3-myc*^{13} P_{BAT2} *leu3cis*Δ (A), or *GCN4-myc*^{13} and *GCN4-myc*^{13} *leu3*Δ (B) (Table 1). Strains were grown on MM with 2% glucose with glutamine (7 mM) as sole nitrogen sources to an OD_{600} 0.5. Binding of WT (solid bars) and mutants (shaded bars) was analyzed by qChIP as described in *Materials and Methods*. IP/input ratios were normalized with the *GRS1* promoter as negative control, and *ILV5* or *HIS4* promoter was used as positive control. Data are presented as the average of three independent experiments along with the SEM. (C and D) Northern blot analysis was carried out on total RNA samples obtained from WT strain and its isogeneic derivatives *leu3*Δ, *gcn4*Δ, and *gcn4*Δ *leu3*Δ double mutant (C), or *ure2*Δ and *gln3*Δ *ure2*Δ double mutant (D) (Table 1). Strains were grown to OD_{600} 0.5 on MM with 2% glucose with glutamine (7 mM) as sole nitrogen sources. Filters were sequentially probed with *BAT2* and *HIS4* or *DAL5* PCR products described in *Materials and Methods*. A 1500-bp *ACT1* PCR fragment was used as loading control. Numbers represent means of *BAT1*/*BAT2* signals normalized to those of *ACT1*, and the resulting ratios in the mutants normalized to those in the WT under derepressing conditions for each gene. SD was found to be ±0.10–0.12.

deprivation (Hinnebusch and Fink 1983). To further support this proposition, the Gcn4-*myc*^{13} strain was constructed and Gcn4 immunoprecipitation was analyzed in a wild-type strain and in a *leu3*Δ mutant (Figure 7B). Gcn4 immunoprecipitation was increased sevenfold in a *leu3*Δ mutant background, indicating a higher Gcn4 content. The fact that, in both the *leu4*Δ *leu9*Δ double mutant and the *leu4*Δ *leu9*Δ *leu1*Δ triple mutant (Figure 6A), decreased or null α-IPM biosynthesis did not result in *BAT2* derepression as it occurs in a *leu3*Δ mutant (Figure 5A and Figure 6B) can be explained, since both the double and triple mutants are leucine auxotrophs and have to be grown in the presence of leucine. In all organisms from yeasts to mammals, the TORC1 pathway controls growth in response to nutrients such as leucine. This amino acid is capable of activating TORC1 kinase, resulting in *GCN4* repression and prevention of TOR-dependent m*GCN4* translation (Valenzuela *et al.* 2001; Kingsbury *et al.* 2015; Kerkhoven *et al.* 2017). This contention is also supported by the herein presented observation that, in the presence of VIL, Gcn4-*myc*^{13} is poorly immunoprecipitated to the *BAT1* and *HIS4* promoters (Figure 4C) as compared to that observed on glutamine or GABA, suggesting a low Gcn4 concentration when cells are grown on VIL.

The fact that *BAT2* expression was repressed on glutamine and induced on VIL suggested it could be an NCR-regulated gene (Courchesne and Magasanik 1988; Minehart and Magasanik 1991; Blinder and Magasanik 1995; Coffman *et al.* 1995). Considering that genes subjected to NCR control are negatively regulated by Ure2, we analyzed whether this factor played a role in *BAT2* expression. As Figure 7D shows, *BAT2* glutamine-dependent repression was alleviated in an *ure2*Δ mutant. In a double *gln3*Δ *ure2*Δ mutant, derepression was not observed, indicating that Ure2-mediated expression is dependent on Gln3, corresponding to an NCR transcriptional regulation profile (Figure 7D). As control, we measured *DAL5* expression, which is a classical NCR-regulated

Table 2 Amino acid deprivation is observed in a *leu3*Δ mutant grown on glutamine as sole nitrogen source

	Amino acid pool (nmol × 10^8 cells)			
	OD_{600} 0.3		OD_{600} 0.6	
	Wild type	*leu3*Δ	Wild type	*leu3*Δ
Valine	1.4	0.64	0.71	0.97
Isoleucine	0.62	0.51	0.41	0.57
Leucine	1.07	0.73	0.69	0.72
Glutamic acid	30.63	8.89	16.26	15.25
Alanine	25.08	5.99	13.58	6.39
Histidine	8.21	4.09	4.23	5.74
Asparagine	0.39	0.43	0.25	0.43
Arginine	1.91	2.44	1.37	2.62
Lysine	1.77	4.5	1.22	9
Tryptophan	0.23	0.23	0.19	0.17

gene. As expected, *DAL5* glutamine-dependent repression was prevented in an *ure2*Δ mutant and hampered in a *gln3*Δ *ure2*Δ double mutant (Figure 7D).

Under catabolic conditions (VIL) Put3 hinders BAT1 expression through a negative indirect effect and activates BAT2 expression

The results presented above (Figure 5A) indicate that Put3 can act as either a positive (*BAT2*) or negative (*BAT1*) regulatory factor, adding a previously unknown function for Put3 as a transcriptional activator (Brandriss 1987). Put3 regulates genes involved in proline utilization, it is constitutively bound to the *PUT1* and *PUT2* promoters, independently of the nitrogen source (Brandriss 1987). However, it only upregulates those genes in the presence of proline or other secondary nitrogen sources, eliciting conformational changes which influence the activation role of Put3 (Axelrod *et al.* 1991). In addition, Put3 regulates transcription by undergoing differential phosphorylation as a function of the nitrogen source quality, improving its ability to activate its target genes (Huang and Brandriss 2000). Our results indicate that the negative action of Put3 on *BAT1* is indirect, since it does not bind the *BAT1* promoter (Figure 5C) and a mutant affecting the Put3-binding, *cis*-acting elements do not result in *BAT1* derepression (Figure 5E). It could thus be considered that while Put3 directly activates *BAT2* expression, its role as a negative modulator of *BAT1* is exerted indirectly. Considering that since Leu3–α-IPM is the main *BAT1* transcriptional activator under biosynthetic conditions and that it could constitute the positive signal activating *BAT1* in a *put3*Δ strain, a *put3*Δ *leu3*Δ double mutant was constructed as described in *Materials and Methods*. Northern blot analysis of *BAT1* on total RNA samples prepared from cells grown on VIL as sole nitrogen source showed that Put3-dependent *BAT1* derepression was not observed in the double *put3*Δ *leu3*Δ mutant (Figure 8A). Thus, the Put3-dependent *BAT1* repression pattern is the result of a lack of Leu3–α-IPM. This indicates that, in a *put3*Δ single mutant, an α-IPM biosynthetic pathway should be operating to allow formation of the Leu3–α-IPM activator. As Figure 8A shows, in a *put3*Δ mutant, *LEU1* and *LEU2* are also derepressed and, as for *BAT1*, this derepression is Leu3 dependent. These data suggest that in a *put3*Δ mutant, in the presence of VIL, leucine could be metabolized to α-IPM through the consecutive action of Bat2-Leu2-Leu1 (Figure 1), enabling Leu3–α-IPM formation and thus recovering the role of Leu3 as a transcriptional activator.

To address the question of the mechanism determining the negative role of Put3 on VIL, it could be considered that since *LEU1* bears a canonical Put3-binding, *cis*-acting element (Figure S6), its expression could be negatively regulated by Put3, and thus in a *put3*Δ mutant, *LEU1* expression would be enhanced. It has been shown that the *LEU1*-encoded IPM isomerase can reversibly determine α-IPM biosynthesis (Kohlhaw 1988). This could allow the formation of Leu3–α-IPM, influencing *LEU2* activation and promoting leucine-dependent Bat2-Leu2-Leu1

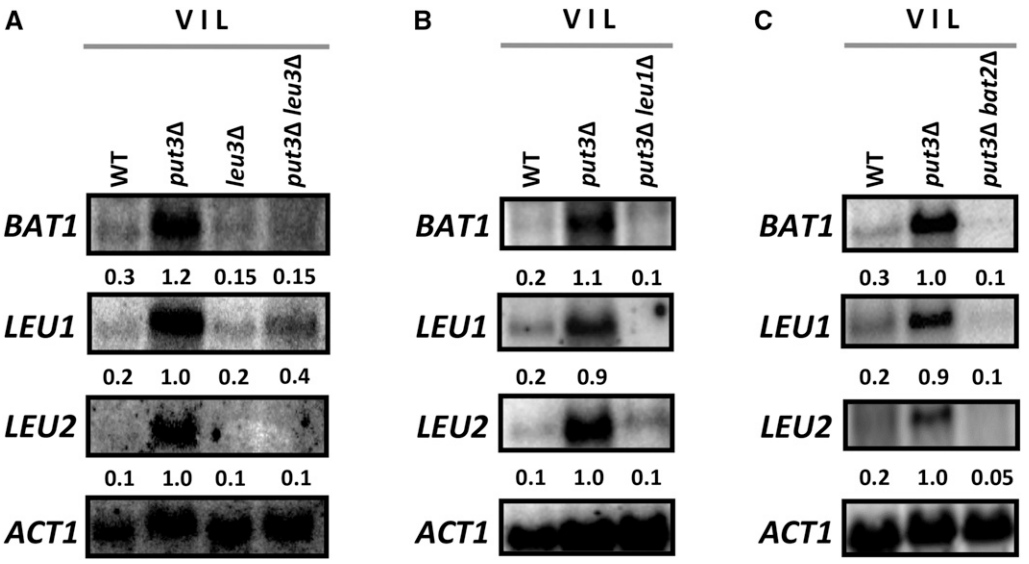

Figure 8 *BAT1* expression is indirectly determined by Put3. (A, B, and C) Northern blot analysis was carried out on total RNA samples obtained from wild-type (WT) strain and its isogeneic derivatives *put3*Δ, *leu3*Δ, *put3*Δ *leu3*Δ, *put3*Δ *leu1*Δ, or *put3*Δ *bat2*Δ double mutant (Table 1). Strains were grown to OD_{600} 0.5 on MM with 2% glucose with valine (150 mg/liter) plus isoleucine (30 mg/liter) plus leucine (100 mg/liter) (VIL) as sole nitrogen sources. Filters were sequentially probed with *BAT1*, *LEU1*, and *LEU2* PCR products as described in *Materials and Methods*. A 1500-bp *ACT1* DNA PCR fragment was used as loading control. Numbers represent means of *BAT1*/*BAT2* signals normalized to those of *ACT1*, and the resulting ratios in the mutants normalized to those in the WT under derepressing conditions for each gene. SD was found to be ±0.10–0.12.

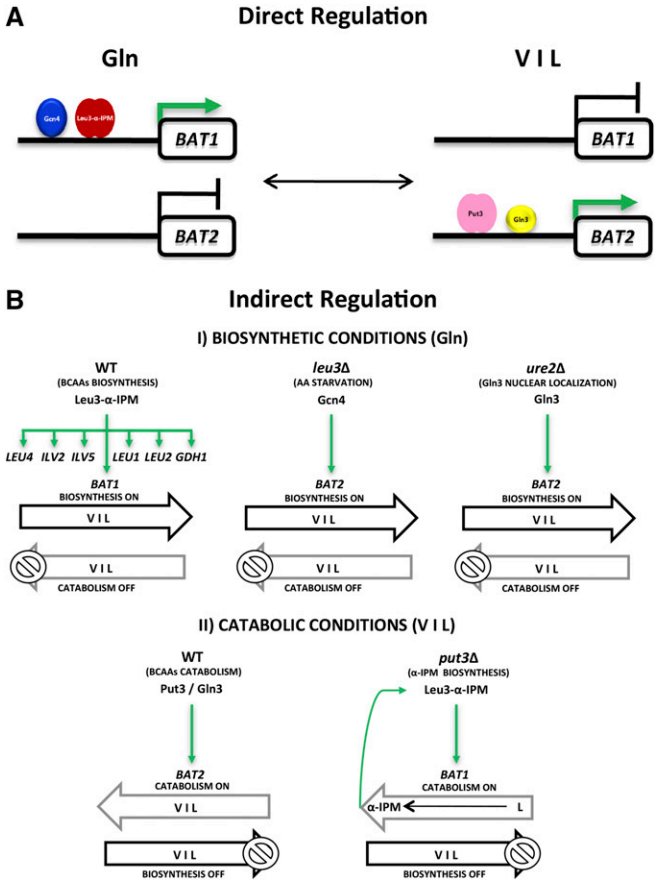

Figure 9 Schematic representation of the *BAT1* and *BAT2* regulatory expression profile depicting TFs acting directly or indirectly on biosynthetic and catabolic conditions. (A) Transcriptional factors with direct regulation on *BAT1*/*BAT2* expression in glutamine (Gln) or VIL as nitrogen sources. Green arrow on *BAT1* and *BAT2* loci (rectangles) indicates transcriptional activation. (B) Different scenarios for the biosynthesis or catabolism of BCAAs in the wild type (WT) and various mutants when grown on biosynthetic (Gln) or catabolic (VIL) conditions. Green arrows pointing down indicate target gene activation through action of transcription factors. Horizontal black or gray arrows indicate VIL biosynthesis or catabolism. This figure highlights the fact that, in a *put3*Δ mutant in the presence of VIL, leucine is preferentially catabolized to α-IPM and not to α-ketoisocaproate (KIC) through the Bat2-Leu2-Leu1 pathway, while valine and isoleucine are catabolized to α-ketoisovalerate (KIV) or α-ketomethylvalerate (KMV) (see Figure 1).

α-IPM biosynthesis. To test this possibility, *put3*Δ *leu1*Δ and *put3*Δ *bat2*Δ double mutants were constructed as described in *Materials and Methods*. As Figure 8, B and C, shows, in these double mutants neither *BAT1* nor *LEU2* were derepressed, indicating that Leu1 and Bat2 activities are required for the functioning of the VIL-insensitive, α-IPM biosynthetic pathway. It is worth mentioning the fact that the results presented above indicate that, on VIL, Put3 can act as either a positive (*BAT2*) or negative (*LEU1*) modulator; however, the mechanisms underlying this Put3 dual role remain to be addressed.

In conclusion, when VIL is present as sole nitrogen source, Put3 determines transcriptional activation of *BAT2*; while it exerts an indirect, negative effect on *BAT1* expression by preventing Leu3-dependent, *BAT1*-induced expression.

Taken together, the results presented above indicate that *BAT1* and *BAT2* have functionally diverged through subfunctionalization of transcriptional regulation, under biosynthetic and catabolic conditions.

Discussion

Aminotransferases constitute an interesting model for studying diversification of paralogous genes carrying out two functions, both of which are needed to warrant metabolite provision, and which cannot be differentially improved to carry out either biosynthesis or catabolism, since aminotransferases constitute biosynthetic and catabolic pathways whose opposed action relies on a single catalytic site (Kohlhaw 1988, 2003). After duplication, *S. cerevisiae* retained the *BAT1* and *BAT2* paralogous pair encoding BCATs, and functional diversification was achieved through differential expression of the paralogous gene pair (Colón *et al.* 2011).

The results presented in this article indicate that *BAT1* and *BAT2* retention and regulatory diversification has promoted the acquisition of two independent systems, which respond to the metabolic status of the cell: the activation of *BAT1* expression through Leu3–α-IPM is indirectly determined by a leucine-sensitive and leucine-independent pathway for α-IPM biosynthesis, while *BAT2* expression is determined by the quality of the nitrogen source (Gln3) and amino acid availability (Gcn4) (Figure 9).

This study analyzes the roles of *cis*- and *trans*-acting elements generating the *BAT1*-biosynthetic and *BAT2*-catabolic expression profiles, the influence of chromatin organization on the expression profiles of *BAT1* and *BAT2*, and the impact of the cell metabolic status triggering expression.

Leucine-sensitive and leucine-resistant independent α-IPM biosynthetic pathways determine the role of Leu3 as an activator or repressor and the biosynthetic expression profile of BAT1

The role of Leu3 on *BAT1* transcriptional activation depends on the biosynthesis and intracellular concentration of α-IPM, which determines whether Leu3 would function as a repressor (Leu3) or an activator (Leu3–α-IPM) (Wang *et al.* 1999; Chin *et al.* 2008). To this end, two α-IPM biosynthetic pathways contribute to the building up of an α-IPM pool. In the absence of VIL, Leu4 and Leu9 play the major role, while in the presence of VIL and in a *put3*Δ genetic background, the consecutive action of Bat2-Leu2-Leu1 determines α-IPM biosynthesis (Figure 1). When VIL is provided, α-IPM biosynthesis through Leu4-Leu4 or Leu4-Leu9 α-IPMS is precluded, limiting the activation capacity of Leu3 (Wang *et al.* 1999; Chin *et al.* 2008; López *et al.* 2015). *BAT1* VIL-dependent repression could be regarded as a determinant mechanism regulating leucine biosynthesis. To further enhance the Leu3–α-IPM-dependent transcriptional activation of *BAT1*, chromatin configuration favors the localization of the Leu3-binding *cis*-acting element on the NFR in this promoter.

Results presented in this article show that in *S. cerevisiae*, an alternative α-IPM biosynthetic pathway can operate through the concerted action of Bat2-Leu2-Leu1, which constitutes a

leucine catabolic pathway and results in VIL-insensitive, α-IPM biosynthesis (Figure 1). Functioning of this pathway occurs only in a *put3*Δ mutant in which repression of *LEU1* is removed, since in this genetic background the *LEU1*-encoded reversible enzyme can catalyze α-IPM biosynthesis from β-IPM (Figure 1) (Kohlhaw 1988; Yang *et al.* 2005). Consequently, the formation of the Leu3–α-IPM complex activates *LEU2* and *BAT1* expression. Accordingly, the expression of *BAT1*, *LEU1*, and *LEU2* is not derepressed in the double *put3*Δ *leu3*Δ mutant (Figure 8A) nor in the *put3*Δ *bat2*Δ double mutants (Figure 8C).

Quality of the nitrogen source and amino acid availability determine the biosynthetic or catabolic expression profile of BAT2

In the *BAT2* promoter, the *LEU3* binding site is occluded by the nucleosome when the strain is grown on either VIL or glutamine as nitrogen sources; however, the *GLN3* and *GCN4* binding sites are accessible on VIL, and protected on glutamine (Figure 3B). *BAT2* is regulated through a glutamine-dependent negative regulatory control, which can be relieved in the presence of secondary nitrogen sources such as VIL. Under these conditions, Gln3 is located in the nucleus and thus able to activate the expression of genes whose products have a compelling role in the catabolism of secondary nitrogen sources such as VIL (Courchesne and Magasanik 1988; Minehart and Magasanik 1991; Blinder and Magasanik 1995; Coffman *et al.* 1995). Additionally, a NCR control-independent mechanism also contributes to *BAT2* repression under biosynthetic conditions (glutamine as sole nitrogen source). In a *leu3*Δ mutant strain, amino acid deprivation is elicited, resulting in Gcn4-enhanced translation thus inducing *BAT2* expression under biosynthetic conditions (Figure 9). Accordingly, in a *gcn4*Δ *leu3*Δ double mutant, neither *BAT2* nor *HIS4* derepression was observed (Figure 7C). Thus, the *BAT2*-restricted transcriptional activation on primary nitrogen sources limits the biosynthetic role of Bat2. However, the independent action of the Gln3 (catabolic) and Gcn4 (biosynthetic) regulators can activate *BAT2*, indicating that the quality of the nitrogen sources and the intrinsic variation of amino acid availability trigger *BAT2* expression and Bat2-dependent VIL biosynthesis (Figure 9). Bat1 and Bat2 could redundantly determine VIL biosynthesis through either Leu3 and/or Gln3/Gcn4 transcriptional activation, since in the presence of secondary nitrogen sources the concurrent action of Gln3 and Gcn4 would increase expression of *BAT2*. The most important fact is that Bat2 can play a role on either VIL biosynthesis or degradation and the only constraint would be *BAT2* mRNA synthesis and translation.

In the presence of a secondary nitrogen source, VIL biosynthesis could be triggered through the concerted action of Bat1 and Bat2, which represents a gene dosage advantage allowing higher biosynthetic capacity. Thus, the acquisition of regulatory systems which allow *BAT1* and *BAT2* expression under biosynthetic and catabolic conditions offers the possibility that Bat1 and Bat2 can play a biosynthetic or catabolic role, depending on the reactant intracellular concentration.

Acknowledgments

We thank Harald Berger and Christoph Schüller for sharing valuable knowledge; Javier Montalvo-Arredondo, Beatriz Aguirre-López, Juan Carlos Martínez Morales, and Eva Klopf for helpful technical assistance; and Rocio Romualdo Martínez for secretarial support. This study was performed in partial fulfillment of the requirements for J.G.'s Ph.D. degree in Biochemical Sciences at the Universidad Nacional Autónoma de México, which wascarried with a Consejo Nacional de Ciencia y Tecnología doctoral fellowship. This project was supported by Dirección de Asuntos del Personal Académico grant/award number IN201015 and by Consejo Nacional de Ciencia y Tecnología grant/award number CB-2014-239492-B.

Author contributions: J.G. and A.G. conceived and designed the experiments; J.G., G.L., S.A., M.e.H., and C.C.-B. conducted experiments; J.G., X.E.-F., J.S., L.R.-R., and A.G. analyzed the data; L.R.-R. and J.S. contributed reagents/materials/analysis tools; J.G. and A.G. wrote the manuscript.

Literature Cited

Avendaño, A., L. Riego, A. DeLuna, C. Aranda, G. Romero *et al.*, 2005 Swi/SNF-GCN5-dependent chromatin remodelling determines induced expression of *GDH3*, one of the paralogous genes responsible for ammonium assimilation and glutamate biosynthesis in *Saccharomyces cerevisiae*. Mol. Microbiol. 57: 291–305.

Axelrod, J. D., J. Majors, and M. C. Brandriss, 1991 Proline-independent binding of *PUT3* transcriptional activator protein detected by footprinting in vivo. Mol. Cell. Biol. 11: 564–567.

Biddick, R. K., G. L. Law, and E. T. Young, 2008 Adr1 and Cat8 mediate coactivator recruitment and chromatin remodeling at glucose-regulated genes. PLoS One 3: e1436.

Blinder, D., and B. Magasanik, 1995 Recognition of nitrogen-responsive upstream activation sequences of *Saccharomyces cerevisiae* by the product of the *GLN3* gene. J. Bacteriol. 177: 4190–4193.

Boer, V. M., J. M. Daran, M. J. Almering, J. H. de Winde, and J. T. Pronk, 2005 Contribution of the *Saccharomyces cerevisiae* transcriptional regulator Leu3p to physiology and gene expression in nitrogen- and carbon-limited chemostat cultures. FEMS Yeast Res. 5: 885–897.

Brandriss, M. C., 1987 Evidence for positive regulation of the proline utilization pathway in *Saccharomyces cerevisiae*. Genetics 117: 429–435.

Byrne, K. P., and K. H. Wolfe, 2005 The yeast gene order browser: combining curated homology and syntenic context reveals gene fate in polyploid species. Genome Res. 15: 1456–1461.

Bysani, N., J. R. Daugherty, and T. G. Cooper, 1991 Saturation mutagenesis of the UASNTR (GATAA) responsible for nitrogen catabolite repression-sensitive transcriptional activation of the allantoin pathway genes in *Saccharomyces cerevisiae*. J. Bacteriol. 173: 4977–4982.

Chin, C. S., V. Chubukov, E. R. Jolly, J. DeRisi, and H. Li, 2008 Dynamics and design principles of a basic regulatory architecture controlling metabolic pathways. PLoS Biol. 6: e146.

Coffman, J. A., R. Rai, and T. G. Cooper, 1995 Genetic evidence for Gln3p-independent, nitrogen catabolite repression-sensitive gene expression in *Saccharomyces cerevisiae*. J. Bacteriol. 177: 6910–6918.

Colón, M., F. Hernández, K. López, H. Quezada, J. González *et al.*, 2011 *Saccharomyces cerevisiae* Bat1 and Bat2 Aminotransferases

have functionally diverged from the ancestral-like *Kluyveromyces lactis* orthologous enzyme. PLoS One 6: e16099.
Conant, G. C., and K. H. Wolfe, 2008 Turning a hobby into a job: how duplicated genes find new functions. Nat. Rev. Genet. 9: 938–950.
Courchesne, W. E., and B. Magasanik, 1988 Regulation of nitrogen assimilation in *Saccharomyces cerevisiae*: roles of the *URE2* and *GLN3* genes. J. Bacteriol. 170: 708–713.
De Boer, C. G., and T. R. Hughes, 2012 YeTFaSCo: a database of evaluated yeast transcription factor sequence specificities. Nucleic Acids Res. 40: D169–D179.
DeLuna, A., A. Avendaño, L. Riego, and A. Gonzalez, 2001 NADP-glutamate dehydrogenase isoenzymes of *Saccharomyces cerevisiae*. Purification, kinetic properties, and physiological roles. J. Biol. Chem. 276: 43775–43783.
Eden, A., L. Van Nedervelde, M. Drukker, N. Benvenisty, and A. Debourg, 2001 Involvement of branched-chain amino acid aminotransferases in the production of fusel alcohols during fermentation in yeast. Appl. Microbiol. Biotechnol. 55: 296–300.
Friden, P., and P. Schimmel, 1988 *LEU3* of *Saccharomyces cerevisiae* activates multiple genes for branched-chain amino acid biosynthesis by binding to a common decanucleotide core sequence. Mol. Cell. Biol. 8: 2690–2697.
Goldstein, A. L., and J. H. McCusker, 1999 Three new dominant drug resistance cassettes for gene disruption in *Saccharomyces cerevisiae*. Yeast 15: 1541–1553.
Gu, X., Z. Zhang, and W. Huang, 2005 Rapid evolution of expression and regulatory divergences after yeast gene duplication. Proc. Natl. Acad. Sci. USA 102: 707–712.
Gu, Z., S. A. Rifkin, K. P. White, and W. H. Li, 2004 Duplicate genes increase gene expression diversity within and between species. Nat. Genet. 36: 577–579.
Guarente, L., B. Lalonde, P. Gifford, and E. Alani, 1984 Distinctly regulated tandem upstream activation sites mediate catabolite repression of the *CYC1* gene of *S. cerevisiae*. Cell 36: 503–511.
Hernández, H., C. Aranda, G. López, L. Riego, and A. González, 2011 Hap2–3-5-Gln3 determine transcriptional activation of *GDH1* and *ASN1* under repressive nitrogen conditions in the yeast *Saccharomyces cerevisiae*. Microbiology 157: 879–889.
Hinnebusch, A. G., 1984 Evidence for translational regulation of the activator of general amino acid control in yeast. Proc. Natl. Acad. Sci. USA 81: 6442–6446.
Hinnebusch, A. G., 2005 Translational regulation of *GCN4* and the general amino acid control of yeast. Annu. Rev. Microbiol. 59: 407–450.
Hinnebusch, A. G., and G. R. Fink, 1983 Positive regulation in the general amino acid control of *Saccharomyces cerevisiae*. Proc. Natl. Acad. Sci. USA 80: 5374–5378.
Hu, Y., T. G. Cooper, and G. B. Kohlhaw, 1995 The *Saccharomyces cerevisiae* Leu3 protein activates expression of *GDH1*, a key gene in nitrogen assimilation. Mol. Cell. Biol. 15: 52–57.
Huang, H. L., and M. C. Brandriss, 2000 The regulator of the yeast proline utilization pathway is differentially phosphorylated in response to the quality of the nitrogen source. Mol. Cell. Biol. 20: 892–899.
Infante, J. J., G. L. Law, and E. T. Young, 2012 Analysis of nucleosome positioning using a nucleosome-scanning assay. Methods Mol. Biol. 833: 63–87.
Ito, H., Y. Fukuda, K. Murata, and A. Kimura, 1983 Transformation of intact yeast cells treated with alkali cations. J. Bacteriol. 153: 163–168.
Kellis, M., B. W. Birren, and E. S. Lander, 2004 Proof and evolutionary analysis of ancient genome duplication in the yeast *Saccharomyces cerevisiae*. Nature 428: 617–624.
Kerkhoven, E. J., Y. Kim, A. Wei, C. D. Nicora, T. L. Fillmore *et al.*, 2017 Leucine biosynthesis is involved in regulating high lipid accumulation in *Yarrowia lipolytica*. MBio 8: 1–12.
Kingsbury, J. M., N. D. Sen, and M. E. Cardenas, 2015 Branched-chain aminotransferases control TORC1 signaling in *Saccharomyces cerevisiae*. PLOS Genet. 11: e1005714.
Kispal, G., H. Steiner, D. A. Court, B. Rolinski, and R. Lill, 1996 Mitochondrial and cytosolic branched-chain amino acid transaminases from yeast, homologs of the *myc* oncogene-regulated Eca39 protein. J. Biol. Chem. 271: 24458–24464.
Kohlhaw, G. B., 1988 Beta-isopropylmalate dehydrogenase from yeast. Methods Enzymol. 166: 429–435.
Kohlhaw, G. B., 2003 Leucine biosynthesis in fungi: entering metabolism through the back door. Microbiol. Mol. Biol. Rev. 67: 1–15.
Leach, L. J., Z. Zhang, C. Lu, M. J. Kearsey, and Z. Luo, 2007 The role of *cis*-regulatory motifs and genetical control of expression in the divergence of yeast duplicate genes. Mol. Biol. Evol. 24: 2556–2565.
Litt, M. D., M. Simpson, M. Gaszner, C. D. Allis, and G. Felsenfeld, 2001 Correlation between histone lysine methylation and developmental changes at the chicken β-globin locus. Science 293: 2453–2455.
Longtine, M. S., A. McKenzie, D. J. Demarini, N. G. Shah, A. Wach *et al.*, 1998 Additional modules for versatile and economical PCR-based gene deletion and modification in *Saccharomyces cerevisiae*. Yeast 14: 953–961.
López, G., H. Quezada, M. Duhne, J. González, M. Lezama *et al.*, 2015 Diversification of paralogous α-isopropylmalate synthases by modulation of feedback control and hetero-oligomerization in *Saccharomyces cerevisiae*. Eukaryot. Cell 14: 564–577.
Makova, K. D., and W. H. Li, 2003 Divergence in the spatial pattern of gene expression between human duplicate genes. Genome Res. 13: 1638–1645.
Marcet-Houben, M., and T. Gabaldón, 2015 Beyond the whole-genome duplication: phylogenetic evidence for an ancient interspecies hybridization in the baker's yeast lineage. PLoS Biol. 13: 8.
Martínez-Montañés, F., A. Rienzo, D. Poveda-Huertes, A. Pascual-Ahuir, and M. Proft, 2013 Activator and repressor functions of the Mot3 transcription factor in the osmostress response of *Saccharomyces cerevisiae*. Eukaryot. Cell 12: 636–647.
Mewes, H. W., K. Albermann, M. Bahr, D. Frishman, A. Gleisner *et al.*, 1997 Overview of the yeast genome. Nature 387: 7–65.
Minehart, P. L., and B. Magasanik, 1991 Sequence and expression of *GLN3*, a positive nitrogen regulatory gene of *Saccharomyces cerevisiae* encoding a protein with a putative zinc finger DNA-binding domain. Mol. Cell. Biol. 11: 6216–6228.
Montalvo-Arredondo, J., Á. Jiménez-Benítez, M. Colón-González, J. González-Flores, M. Flores-Villegas *et al.*, 2015 Functional roles of a predicted branched chain aminotransferase encoded by the *LkBAT1* gene of the yeast *Lachancea kluyveri*. Fungal Genet. Biol. 85: 71–82.
Ohno, S., 1970 *Evolution by Gene Duplication*. Springer-Verlag, New York.
Quezada, H., C. Aranda, A. DeLuna, H. Hernández, M. L. Calcagno *et al.*, 2008 Specialization of the paralogue *LYS21* determines lysine biosynthesis under respiratory metabolism in *Saccharomyces cerevisiae*. Microbiology 154: 1656–1667.
Rawal, Y., H. Qiu, and A. G. Hinnebusch, 2014 Accumulation of a threonine biosynthetic intermediate attenuates general amino acid control by accelerating degradation of Gcn4 via Pho85 and Cdk. PLoS Genet. 10: 7.
Sheff, M. A., and K. S. Thorn, 2004 Optimized cassettes for fluorescent protein tagging in *Saccharomyces cerevisiae*. Yeast 21: 661–670.
Siddiqui, A. H., and M. C. Brandriss, 1989 The *Saccharomyces cerevisiae PUT3* activator protein associates with proline-specific upstream activation sequences. Mol. Cell. Biol. 9: 4706–4712.
Storci, F., and M. A. Resnick, 2003 *Delitto perfetto* targeted mutagenesis in yeast with oligonucleotides. Genet. Eng. 25: 189–207.

Struhl, K., and R. W. Davis, 1981 Transcription of the *his3* gene region in *Saccharomyces cerevisiae*. J. Mol. Biol. 152: 535–552.
Sze, J. Y., M. Woontner, J. A. Jaehning, and G. B. Kohlhaw, 1992 *In vitro* transcriptional activation by a metabolic intermediate: activation by Leu3 depends on α-isopropylmalate. Science 258: 1143–1145.
Thomas-Chollier, M., O. Sand, J. V. Turatsinze, R. Janky, M. Defrance *et al.*, 2008 RSAT: regulatory sequence analysis tools. Nucleic Acids Res. 36: W119–W127.
Thomas-Chollier, M., M. Defrance, A. Medina-Rivera, O. Sand, C. Herrmann *et al.*, 2011 RSAT 2011: regulatory sequence analysis tools. Nucleic Acids Res. 39: W86–W91.
Turatsinze, J. V., M. Thomas-Chollier, M. Defrance, and J. Van Helden, 2008 Using RSAT to scan genome sequences for transcription factor binding sites and *cis*-regulatory modules. Nat. Protoc. 3: 1578–1588.
Valenzuela, L., P. Ballario, C. Aranda, P. Filetici, and A. González, 1998 Regulation of expression of *GLT1*, the gene encoding glutamate synthase in *Saccharomyces cerevisiae*. J. Bacteriol. 180: 3533–3540.
Valenzuela, L., C. Aranda, and A. González, 2001 TOR modulates GCN4-dependent expression of genes turned on by nitrogen limitation. J. Bacteriol. 183: 2331–2334.
Van Helden, J., 2003 Regulatory sequence analysis tools. Nucleic Acids Res. 31: 3593–3596.
Wang, D., F. Zheng, S. Holmberg, and G. B. Kohlhaw, 1999 Yeast transcriptional regulator Leu3p: self-masking, specificity of masking, and evidence for regulation by the intracellular level of Leu3p. J. Biol. Chem. 274: 19017–19024.
Wolfe, K. H., and D. C. Shields, 1997 Molecular evidence for an ancient duplication of the entire yeast genome. Nature 387: 708–713.
Yang, C. R., B. E. Shapiro, S. P. Hung, E. D. Mjolsness, and G. W. Hatfield, 2005 A mathematical model for the branched chain amino acid biosynthetic pathways of *Escherichia coli* K12. J. Biol. Chem. 280: 11224–11232.
Zhang, J., 2003 Evolution by gene duplication: an update. Trends Ecol. Evol. 18: 292–298.
Zhang, Z., J. Gu, and X. Gu, 2004 How much expression divergence after yeast gene duplication could be explained by regulatory motif evolution? Trends Genet. 20: 403–407.
Zhou, H., and F. Winston, 2001 *NRG1* is required for glucose repression of the *SUC2* and *GAL* genes of *Saccharomyces cerevisiae*. BMC Genet. 2: 5.

Communicating editor: A. Hinnebusch